Path loss Exponent

In wireless communication, the path loss exponent has a strong impact on the quality of links or signal, and hence, there are needs to accurately estimate the efficient design and operation of wireless network. Many research efforts have been devoted to modeling the path loss propagation effects for narrowband communication by using different methods ranging from analytical models, semi-empirical models, to empirical models. Telecommunication industries today have a major problem which is losses that occur during transmission of signals from the transmitter to the receiver. In this thesis, the empirical method was adopted though it is so stressful because it involves the measurement of large data, with the help of a software called RF signal tracker which was installed in a mobile phone called Samsung galaxy pocket, this software gave us the distance to site and the signal strength level of the network provider at a particular distance. A fixed distance was taken from the base station to the receiver and in this research work a particular fixed distance was taken as 100m from the base station which was represented as d0 and a variable distance which was represented as this.
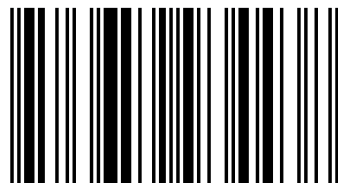
Stanley Uzairue

I am UZAIRUE Stanley with Bachelor Degree in Elect/Elect Engineering and Masters Degree in Electronics and Telecommunication Engineering from Ambrose Alli University,Nigeria; Executive Masters in Project Management from Cupe Business School, United Kingdom. Presently Head, Fibre-To-The-X network design, implementation and operations, Swift Networks

Determination and Analysis of Signal Strength/Path-Loss Exponent

ISBN 978-3-659-93443-8

Uzairue

LAP LAMBERT Academic Publishing

Stanley Uzairue

Determination and Analysis of Signal Strength/Path-Loss Exponent

Stanley Uzairue

Determination and Analysis of Signal Strength/Path-Loss Exponent

LAP LAMBERT Academic Publishing

Coverbild / Cover image: www.ingimage.com

DEDICATION

This work is dedicated to God Almighty.

ACKNOWLEDGEMENTS

LIST OF FIGURES

LIST OF ABREVIATIONS

PLE	Path Loss Exponent
MSE	Minimum Square Error
GSM	Global System For Mobile Communication
NCC	Nigeria Communication Commission
PTOs	Private Telephone Operators
CSD	Circuit Switched Data
CCI	Calling Code Identity
HSCSD	Higher Speed Circuit Switched Data
GPRS	General Pocket Radio Data Service
3G	3rd Generation
2G	2nd Generation
CDMA	Code Division Multiple Access
DECT	Digital Enhanced Cordless Telecommunication
WIMAX	Worldwide Interoperability For Microwave Access
UMTS	Universal Mobile Telecommunication System
TX	Transmitter
RX	Receiver
RSS	Received Signal Strength
RF	Radio Frequency
LOS	Line Of Sight
ITU	International Telecommunication Union
UHF	Utra High Frequency

SAM   Simplified Alternation Model

NLOS   Non Line Of Sight

G_t Transmitter Antenna Gain

G_r Receiver Antenna Gain

$PL(d_0)$ Path Loss at Reference Distance d_0

AMU   Median Loss Relative To Free Space

L(dB)   Median Path Loss

LF   Free Space Path Loss

G(ht)   Base Station Gain Factor With Height ht

BS   Base Station

G_{area} Environmental Gain Factor

FWA   Fixed Wireless Access

ECC   Electronic Communication Committee

SUI   Stanford University Interim

P_{TX} Transmitter Output Power

G_{TX} Transmitter Antenna Gain (dBm)

L_{TX} Losses (dBm)

P_{RX} Received Power (dBm)

L_M Miscellaneous Losses (dBm)

PPP   Point to Point Protocol

AAU   Ambrose Alli University, Ekpoma

IMEI   International Mobile Equipment Identity

ESN   Electronic Serial Number

SIM SN   Sim Serial Number

EVDO   Evolution Data Optimized

E_c/I_0 The Ratio Of Received Power Of The Carrier

                To The All Over Noise

SNR   Signal to Noise Ratio

MCC   Mobile Country Code

MNC   Mobile Network Code

LAC   Location Area Code

GPS   Global Positioning System

ABSTRACT

In wireless communication, the path loss exponent has a strong impact on the quality of links or signal, and hence, there are needs to accurately estimate the efficient design and operation of wireless network. Many research efforts have been devoted to modeling the path loss propagation effects for narrowband communication systems by using different methods ranging from analytical models, semi-empirical models, to empirical models. Telecommunication industries today have a major problem which is losses that occur during transmission of signals from the transmitter to the receiver.   In this thesis, the empirical method was adopted though it is so stressful because it involves the measurement of large data, with the help of a software called RF signal tracker which was installed in a mobile phone called Samsung galaxy pocket, this software gave us the distance to site (base station) and the signal strength level of the network provider at a particular distance. A fixed distance was taken from the base station to the receiver and in this research work a particular fixed distance was taken as 100m from the base station which was represented as d_0 and a variable distance which was represented as d_i. From my data, it was observed that the calculation of path loss with log – distance model which is deterministic is not as accurate as the empirical model (generated model), the generated model gave a better and more accurate

result than the existing ones, and that the path loss exponents of the tested locations was fully known. A mathematical model was developed to calculate the power received of GSM signal in Ekpoma and the model was named Anyasi's model". From calculations the path loss exponent values were 1.48, 1.34, 1.11 and 1.48 dBm respectively for the tested locations namely; College of medicine, Ambrose Alli University, Ekpoma, Ujoelen Ekpoma, Eguare Ekpoma and Emaudo Campus, Ambrose Alli University, Ekpoma. Comparing the signal strength obtained from the generated model and the measured signal strength obtained from RF signal tracker, it was observed that they are almost of the same values

LIST OF TABLES

Calculation Of Y (modeled loss constant) For Each Of The Locations For The Research Period.

For college of medicine.

For the Ujoelen, Location

For Eguare, Ekpoma Location

Emuado Campus Aau, Ekpoma Location

Calculation Of Signal Using Uzairue's Generated Model And Generated Loss Constant.

College Of Medicine Campus, AAU, Ekpoma Location

Ujoelen, Ekpoma Location

Eguare Ekpoma Location

Emuado Campus, AAU Ekpoma

Shows The Summary Of The Comparison Between Path Loss Values From Measurement and Using Model Equation

Comparison Between The Path Loss Values From Measurement, Using Deterministic/Theoretical Model (log-distance path loss model) And The Generated Empirical Model (Anyasi's model) For The Period Used ''Ujoelen Ekpoma''.

Comparison Between The Path Loss Values From Measurement, Using Deterministic/Theoretical Model (log-distance path loss model) And The Generated Empirical Model (Anyasi's model) For The Period Used ''Eguare Ekpoma''.

Comparison Between The Path Loss Values From Measurement, Using Deterministic/Theoretical Model (log-distance path loss model) And The Generated Empirical Model (Anyasi's model) For The Period Used ''Emaudo Ekpoma''.

TABLE OF CONTENTS

CHAPTER ONE

INTRODUCTION

1.1. Background of Study

The world is fast becoming a global village and a necessary tool for this process is communication, of which telecommunication is a key player. The quantum advancement in the telecommunication industry all over the world is rapid as one innovation replaces another in a matter of weeks. A major breakthrough is the wireless telephone system which comes in either fixed wireless line or global system for mobile communication (GSM). Without mincing words, communication is a major driver of any economy (Thiago, 2001). In recent years we have witnessed remarkable growth in mobile communication service in Nigeria. The Nigeria telecommunication sector was deregulated under the military regime in 1992 with the establishment of a regulatory body known as the Nigerian Communication Commission (NCC). Since then, the NCC has issued various licenses to private telephone operators (PTOs) for both fixed wireless telephone lines and mobile phones. The return of democracy in 1999 however reviewed the procedure for granting GSM license to three service provider. MTN, ECONET (which is now zain) and NITEL PLC in 2001, with Globacom joining in 2003. The

technological advancement of GSM in the world was prompted by the need to provide seamless telecommunication through Europe. Bolus in 1980, analogue mobile telephony was growing rapidly and operators found it increasingly difficult to interconnect the various networks in Europe. This was so because each implementation of the analogue service was fundamentally different, which made inter-working a serious challenges. To address these challenges, a study group called group special mobile (GSM) was formed. Out of this and seven years later, the GSM standard was realized (Nigerian businessinfo.com, 2003).

Today, GSM cover over 2.5 billion (US census bureau) users on 630 networks in over 210 countries (Nigeria inclusive) and is the fastest growing technology of all time. The initial release of GSM was called GSM phase 1, and is commonly referred to as the first generation, this release made provision for the basic voice, SMS and circuit switched data (CSD) service. CSD allows a maximum data rate of 9.6 kb and was capable of fax transmission as well, supplementary service at that point was very basic consisting of call forward and called barring capabilities (Turmani and Toledo, 2002).

GSM phase 2 termed second generations was released and provided enhanced supplementary service, among which were calling identity (CCI), cell waiting and multiparty service. Data services however remained limited to 9.6 kbs. In so many ways we are celebrating the most significant communication season in the Nigeria history, the improvement cut across the entire industries, and the growth premium started with the introduction of the 1000 units of TAC in 1999 by NITEL in collaboration with Ericson. The processor to the TAC was the "analogue mobile" introduced in 1991. "Between" 2002-2004, the performance of the fixed line and fixed wireless operators had increased by over 31 per cent both in number of lines issued and quality of services. The reconstruction of NITEL into fixed and mobile (MTEL) had brought about two internally efficient companies with greater focus (Ajakaye, 2005).

The first four GSM network operators in Nigeria were MTN, VEX mobile (VMobile) now Zain, Globacom and Mtel have brought significant energy and steam to our national economy, the operators have issued over three million lines within the first two years of operation. The "talking" is an advance of ingredient both for our people and the economy. The PTOs and the various other secondary and value-added

service providers have contributed greatly in making the communication offering a complete package (International Engineering Consortium, 2005).

Nigeria's focus remain technology advancement of the GSM industry and of the Nigeria economy, the interrelationship of the industry has been large and progressive peer check and mediation is the hallmark of dispute resolution in GSM industry at a growth stage, the NCC, to quickly resolve all interconnection issues, not just of voice but also SMS. The NCC set up the consumer complaints bureau and the digital bridge institution, and in nipping the menace of tons who masquerade as value added service providers (Balogun, 2000).

GSM phase 2+ was an enhancement to GSM phase 2 and was released after two years GSM phase 2+ addresses this requirement by making provision for higher speed circuit switched data (HSCSD) and general packet radio data service (GPRS). HSCSD and GPRS allowed maximum data rates of 48 kbs and 177 kbs respectively.

GSM phase 3 termed 3G (3rd generation) allows simultaneous use of speech and data service and higher data rate up to 14.0 mbs on the downlink and 5.8 mbs on the uplink with HSPA. The families' standard

mobile telecommunication union (ITU) is CDMA 2000, DECT and WIMAX. Services include wide area wireless voice telephony, video calls and wireless data, all in mobile environment (Clint and Daniel, 2000).

Universal mobile telecommunication system (UMTS) is one of the 3G technologies which is also being developed on GSM networks beginning in 2003, EDGE is considered as a 3G technology and is part of ITU's 3G definition, EDGE can be used for any package switched application such as internet connection, as well as wimax technology (4G) (ITU, 2009).

In Nigeria, there has been more expectation rolled out in rural areas coverings over 50 % government area and at least 5000 communities and villages. The result of this will be the availabilities of spares capacity that can be utilized by other interest for conveying data, video and voice. This advancement informs Nigeria's present rating as the fastest growing telecommunication market in Africa. There is no doubt that the telecommunication sector has united the whole world within a second, business is on the wheel globally. Nevertheless considering the previous relationship existing questions are now; does this global system for mobile communication have imparted in Nigeria

economy? Does it contribute to job creation and crime reduction? (http://www.allafrica.com, 2009).

As the word is increasing in population developmental activities and technologies increase daily, also problem begins to arise in the communication services, like traffic in system and signals. Low capacity, less coverage area and poor quality of service, telecommunication industries today have a major problem which is losses that occur during transmission of signals from the point of transmission (transmitter) to the receiving end (receiver) (Rappaport, 2002).

1.2. Overview of Radio Wave Propagation
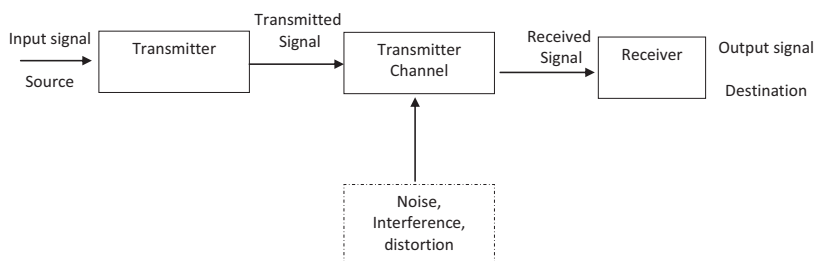
Fig.1.1: A communication system (Carlson et al, 2002)

A typical communication system consists of three main systems: the transmitter (TX), the receiver (RX) and the transmission channel as depicted in Fig.1.1. It is desirable to understand the channel's statistical

characteristics in order to predict the channel behavior. The signal processing techniques then will be developed and used properly to ensure that the transmission channel between the TX and the RX is as reliable as possible. Therefore, understanding the channel characteristics plays an important role in designing and optimizing communication system. The channel is subject to noise, distortion and other interference sources leading to the variation of the received signal power. The models that characterize the signal fluctuations over small distances in the order of the wavelength or short-time duration are called small-scale models. While the propagation models that predict the mean signal strength over the large distances between the TX and the RX or long-time duration are called large-scale or path-loss models. Path loss refers to the signal power lost while a radio wave propagates along a path from the TX to the RX. The total received signal typically fluctuates due to the constructive and destructive addition of multipath signals along various paths of wave propagation (Gordon, 2001).

The three main path-loss mechanisms are described in the following:

• Reflection

When radio wave impinges upon the surface of an object that is large compared to the wavelength, a portion of the incident wave is

reflected off the object and travels in a direction governed by Snell's law of reflection. Snell's law states that the angle of incidence is equal to the angle reflection. The electric field intensity of the reflected wave is related to the incident wave through the reflection coefficient. It is well understood that the reflection coefficient depends on the material characteristics of the media, wave polarization, angle of incident, and wave frequency (McKown and Hamilton, 1991).

• Diffraction

When a radio wave is incident upon an object with an electrically large sharp edge, the wave creeps around the sharp edge into the shadow region of the object by virtue of the propagation mechanism called diffraction. The effect of diffraction is more prominent at high frequencies. Diffraction plays an important role similar to reflection that enables a transmitted radio signal reaching a receiving antenna even in the absence of the direct line of sight between the TX and RX. The diffraction mechanism can be explained by Huygen's principle. According to this principle, every point in a primary wave acts as a point source radiating secondary spherical wavelets. The totality of these secondary spherical wavelets constitutes a secondary wave front of a traveling wave. This is the very mechanism that a radio wave creeps around the

sharp edge of an object and penetrates into the shadow region. Diffraction is clearly important for radio wave propagating in an environment that is occupied by numerous random objects. Naturally, diffraction depends on the edge geometry of obstacles, the propagation medium, and the wave characteristics (Hata and Nagatsu, 1980).

• Scattering

The phenomenon of scattering takes place when a radio wave is incident upon an electrically rough surface. It results in the incident radio wave being bounced off the surface in various directions. The "roughness" of a scattering object refers to the protuberance on its surface. The effect of scattering becomes significant when the 3 protuberance is of the order of the wavelength. In case of reflection, the reflected wave travels in a unique direction dictated by Snell's law. For scattering, the incident wave is reflected in a diffused manner thereby resulting in numerous reflected waves traveling away from the scattering object in different directions within some irregular conical region. In essence, scattering is attributed to rough surfaces or irregularities. Because of scattering, it may happen that the actual signal received is stronger than what is predicted by reflection and diffraction only. The reflection and scattering mechanisms serve as the basis for

developing the path-loss model. The diffraction loss relating to the sharp irregularities of the obstructed surfaces is not taken into account in the proposed model.

1.3. Brief Review of Path-loss models

Many research efforts have been devoted to modeling the path loss propagation effects for narrowband communication systems by using different methods ranging from analytical models, semi-empirical models, to empirical models. An analytical model is typically based on applying electromagnetic theory to a specific environment. Detailed information about the environment needs to be available in order to formulate the model. Thus, an analytical model tends to be precise but complicated to apply. Moreover, it is site-specific. A semi-empirical model starts with a simple physics-based model with unknown parameters. The simple physical model makes it relatively easy to implement but not accurate enough to account for the more complex features of a given environment. The unknown model parameters are to be determined from measurements so as to improve the accuracy of the model. Semi-empirical models are generally site-specific. In practice, most radio propagation path-loss models are semi-empirical models. They are usually developed by fitting parameterized physical models to

measurement data. An empirical model is simply a hypothesized mathematical model determined by fitting measurement data. It may not have any physical basis. However, empirical models are easy to use since they do not require any information about the environment. Numerous measurement-based, narrowband, semi-empirical path-loss models have been proposed and investigated. The path loss for macro cells with coverage areas having radii from 14km to 20 km has been proposed by Hata, and several other research groups (Sams, 1986). Hata proposed the path-loss models for different environments such as urban areas, suburban areas, and rural areas based on measurement data. All of these models are similar with respect to the signal attenuation rate (path loss exponents). Lee also performed measurement works in different cities around the world and proposed alternate path-loss models (Erceg et al, 1999). Those models are applicable not only for different environments, but also for varying carrier frequency, antenna heights, the TX-RX separation, etc. For small distances between the TX and the RX, several other research groups have also proposed the path-loss models for micro-cell areas (Gordon, 2001). It is noticed that all the semi-empirical models predict the median path losses. There are some techniques used to develop the path-loss model using computer

simulation. The two-ray models are most commonly used to predict the path loss and calculate the signal strength. These models use the ray-tracing technique that is based on geometrical optics to account for the three mechanisms discussed above (Anderson, 2001). This technique assumes a finite number of multipath signals from the TX to the RX. The knowledge about the physical elements of the channel is essential, including the geometry of the scattering objects in the channel. To simplify the solution and procedure, however, the ray tracing technique often makes approximations to obtain an excess path length (McKown and Hamilton, 2001). Typically, it is assumed that the nearest scattering objects are in the far-field regions of the TX and the RX. In addition, the scattering objects are electrically large (Schaubach et al, 1992). Several research efforts reported have employed the ray-tracing technique. It shows a simple deterministic-plus-stochastic path-loss model for small outdoor areas (such as parking lots and intersections). It is found that for these areas with well-defined geometries, a model (such as 2-ray, 4-ray or multipath reflection model) may be postulated initially and the corresponding measurement will be performed to verify the accuracy of the assumed models. (Domazetovic et al, 2002).

1.4. Problem Statement

One may notice that the research works described in section 1.3 have several limitations as described in the following:

• The collection and measurement of data are generally very tedious and costly because large volume of data needs to be acquired and specialized expensive equipments are involved.

• The measurement of data is inherently site-specific and varies from site to site.

• The ray tracing technique often makes approximations to obtain excess path lengths.

• Some existing models have been proposed and verified by measurement for very small outdoor areas characterized by the TX-RX separation less than 50 meters. In view of the limitations described above, it is desirable to have a computer simulation model to predict the path loss for different environments and to validate the existing semi-empirical models. To achieve this objective, a computer simulation model was proposed that will require minimal information about the environment. More specifically, only the number of scattering objects and their locations are used to predict the path loss. Such an approach essentially makes the proposed model widely applicable to different

environments. The added benefit is that it does not require the high costs associated with the measurement efforts. Moreover, the computer simulation model may lead to criteria for identifying the proper conditions that are best suited for a specific existing semi-empirical model. To develop a flexible computer model that possesses the attractive features described previously, the following solution approach was taken. Multipath signals resulted from the scattering by any number of randomly located objects are considered. Each multipath signal is a two-hop signal that involves a single scattering object. The wave (signal) interactions between the TX and a scattering object are based on the two-ray model without making restrictive assumptions. The same approach is used to account for the wave interactions between a scattering object and the RX. The two-ray model considers the effects of wave propagation along the direct path as well as the indirect path due to ground reflection. The phase and magnitude of the received signals are taken into account in order to properly understand the received signal characteristics. In addition, the proposed model allows the flexibility in studying the dependence of path loss on the density of scattering objects and the distance between the TX and the RX. The key step in the development of the model is the proper representation of

the electric field due to the direct path and ground-reflected path. The power transmitted from the TX to the objects is absorbed and then reradiate to the RX. The corresponding electric fields at the RX due to the objects are then calculated. Subsequently, the total electric field and power received are then obtained. The path loss exponents and intercepts are yielded by fitting the path losses versus log distance according to the minimum mean-square error criterion. The direct path from the TX to the RX is assumed absent. The rational is that it is very likely that there are always scattering objects blocking the direct path in view of the fact that the distance between the TX and the RX is quite large, ranging from 1 km to 20 km. The preliminary work of this model is reported in (Hung Huy Khong et al, 2008).

In wireless channels, the path loss exponent (PLE) has a strong impact on the quality of links, and hence, it needs to be accurately estimated for the efficient design and operation of wireless networks. In this thesis, the problem of PLE estimation in large wireless networks, which is relevant to several important issues in networked communications such as localization, energy-efficient routing, and channel access was discussed. Large ad hoc network where nodes are distributed as a homogeneous Poisson point process on the plane and

the channels are subject to Nakagami-m fading was considered. The proposed and discussed three distributed algorithms for estimating the PLE under these settings which explicitly take into account the interference in the network. In addition, simulation results to demonstrate the performance of algorithms and quantify the estimation errors were discussed. How to estimate the PLE accurately even in networks with spatially varying PLEs and more general node distributions was discussed (Andrea, 2005).

The wireless channel presents a formidable challenge as a medium for reliable high-rate communication. It is responsible not only for the attenuation of the propagated signal but also causes unpredictable spatial and temporal variations in this loss due to user movement and changes in the environment. In order to capture all these effects, the path loss for RF signals are commonly represented as the product of a deterministic distance component (large-scale path loss) and a randomly-varying component (small-scale fading). The large-scale path loss model assumes that the received signal strength falls off with distance according to a power law, at a rate termed the path loss exponent (PLE). Fading describes the deviations of the received signal strength from the power-law decay due to shadowing and the

constructive and destructive addition of its multipath components. While the small-scale fading behavior of the wireless channel can be well-represented using stochastic processes1, it is critical to accurately estimate the PLE for the efficient design and operation of wireless networks (Remley et al, 2000).

This estimation problem is non-trivial even for a single link due to the existence of multipath propagation and thermal noise. For large wireless networks without infrastructure, the problem is further complicated due to the following reasons: First, the achievable performance of a typical ad hoc or sensor network is not only susceptible to noise and fading, but also to interference due to the presence of simultaneous transmitters (Domazetovic et al, 2002). Dealing with fading and interference simultaneously is a major difficulty in the estimation problem. Second, the distances between nodes themselves are subject to uncertainty. Often, the distribution of the underlying point process can be statistically determined, but precise locations of the nodes are harder to measure. In such cases, there will need to consider the fading and distance ambiguities jointly, i.e., define a spatial point process that incorporates both. In this thesis, the present three distributed algorithms to accurately estimate the channel's PLE for

large wireless networks with uniformly randomly distributed nodes in the presence of fading, noise and interference, based solely on received signal strength measurements. The simulation results to illustrate the performance of the methods and study the estimation error was also provide. Additionally, briefly describe how to accurately estimate the PLE in environments with spatially varying PLE values and for more general node distributions (Chen et al, 2000).

II MOTIVATION AND RELATED WORK

Motivation

In this section, the importance of knowing the PLE for efficient design and operation of wireless networks was shown. Though it is often assumed in analysis and design problems that the value of the PLE is known a priori, this is not true in practice, and hence, the PLE needs to be accurately estimated during the network initialization phase. The PLE estimation problem is closely related to that of localization, which is an integral component of network self-configuration (Rappaport, 2002). When bestowed with the ability to detect their positions, sensor nodes deployed in an ad hoc fashion can support a rich set of geographically aware protocols and accurately report the regions of detected events. Detailed knowledge of the nodes' locations is also needed for

performing energy-efficient routing of packets in the network. An important class of localization algorithms is based on received signal strength (RSS) measurements (Jakes, 1994), but it needs accurate estimates of the PLE to perform well. Another fundamental issue in sensor networks is the sensing problem that deals with how well a target area or a phenomenon can be monitored. Studying network characteristics such as connectivity is important for such applications and requires accurate estimates of the PLE (Patwari et al, 2003). The performance of contention-based systems such as slotted ALOHA is very sensitive to the contention probability p, hence it is critical to choose the optimal operating point of the system. The value of the contention parameter is determined based on various motives such as maximizing the network throughput (Bettstetter.C, 2004) or optimizing the spatial density of progress. These quantities also greatly depend on the PLE, and therefore the optimal value of the contention probability can be chosen only after estimating (Haenggi, 2009).

1.5. Justification for the Study

Considering the losses during transmission of electrical, electronic, microwaves signal from the transmitter to the receiver in our communication/telecommunication industries, and also considering the

importance of these industries in our social, physical life and in the growth of world economy, there are needs to determine the path loss of the signal transmitted from the sending ends to the receiving ends and the penetration level in our home i.e. determining how our house appliances, buildings, trees and other factors affect the signals and with the view of providing the methods in which the losses (path loss) can be minimize (Rappaport, 1996).

The critical problems that are encountered by telecommunication industries in Nigeria have contributed to the down fall of telecommunication industries worldwide and Nigeria included, here are some of the highlighted problems (ITU, 2009).

I.   The GSM problems, which include rejection of calls by networks

II.   Call fading during communication, example in a situation whereby customer on call suddenly experiences reduction in speech volume from the person making the call to the person receiving the call.

III. In the place of internet network, a situation whereby the uplink and downlink suddenly send and receive at a lower rate or no transmission.

Due to these effects and how the communication industries being affected by these effects, there are needs to try as much as possible to eliminate or reduce these drawback that affect our communication industries (Clint and Daniel, 2000).

1.6. Objectives of the Study

1.6.1. Aim of Study

The overall aim of the study is to determine the path loss exponent and signal penetration level in Nigeria, using Ekpoma Edo State as a case study.

1.6.2. The Specific Objectives of the Study:

a) To assess the 3 distributed models to accurately estimate or calculate the channel's path loss exponent for large wireless networks, namely:

    I.   Empirical models

    II.   Semi-deterministic models

    III.   Deterministic models

b) To determine the causes of losses of signals and penetration level.

c) To develop a mathematical model to determine path loss exponent

1.7. Research Methodology

The various methods that were adopted in the realization of this study are:-

I.   Measurement of necessary data with software called RF signal tracker; This software gives the GSM signal strength of the network provider, in this research work a particular network provider was put into consideration (MTN network provider)

II.   This software called RF signal tracker with software version 01 was installed in a mobile phone called Samsung galaxy with the model GT – 55300, see Fig.1.2 for the diagram of the mobile phone and Table (1.1) shows the main menu screen of the software

Device layout

Earpiece

Volume key

Home key

Option key

Touch screen

Back key

Microphone

Multifunction jack

Camera lens

Power/Reset/Lock key

Headset jack

GPS antenna¹

Speaker

Back cover

Main antenna
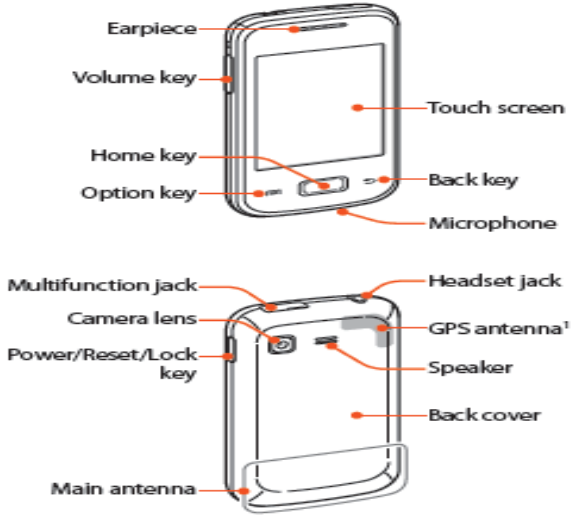
Fig.1.2: Samsung Galaxy Phone Picture

Table 1.1: RF main screen menu

Phone Parameters.	
Number	08063268446
Phone type	GSM
IMEI/ESN	353170055933935
Manufacturer	Samsung
Model	GT-S5300
SIM SN	Nil
SIM State	STATE-READY
Software version	01
Sub ID	Nil
Signal strength	-75dBm
Bit Error Rate	255
EVDO	-1dBm

Ec/I$_o$	-1
SNR	-1
Battery level	80%
Network Parameters	
Operator	MTN
Technology	EDGE
MCC	621
MNC	Nil
LAC	30
Cell id	33061
Location Parameters	
Site database	Google
Best Provider	GPRS
Mobile latitude	$6^0 44' 24.724''$
Mobile longitude	$6^0 6' 28.675$
Mobile Heading	Nil
Mobile Altitude	263m
Site brg	Nil
Speed	Nil
GPS Accuracy	± 26.2ft
Distance to Site	1km

III.   During the measurement of the data with a software called RF signal tracker, the following steps was taken;

- A fixed distance was taking from the base station to the receiver and in this research work a particular fixed distance was taking as 100m from the base station which will be represented as d_0 and a variable distance which was represented as d_i.

- The following parameters was recorded, distance to site and the signal strength of the network, the distance was in kilometer and the signal strength was in decibel.

- The data was measured for six months; this period was taken in order to have a clear picture of the variation of the signal strength based on the distance to site and in order to have a clear analysis of the data measured.

IV. Estimation and analysis of the data collected to know the path loss exponent of a particular area, example (College of medicine AAU, Emaudo campus AAU, Ujoelen and Eguare) all in Ekpoma, Edo State Nigeria.

V. Using Okumura model to determine the signal strength of GSM network; The Okumura model is applied when frequencies range from 150 KHz to 1920 MHz and distances from the TX to the RX, range from 1 km up to 100 km when determining the signal strength. It is mathematically represented as

$L\ (dB) = LF + Amu\ (f,d) - G(ht) - G(hr) - G_{AREA}$

VI. Using Hata model to determine the signal strength of GSM network; Hata further developed the Okumura model from the semi-empirical

path loss data provided by Okumura. The Hata model is mostly applicable for urban areas that have not been addressed in the Okumura model. And it is mathematically represented as

$L(dB) = 69.55 + 26.16\log fMHz - 13.82\log ht - a(hr) + (44.9 - 6.55\log ht)\log dk$

$m - K$

CHAPTER TWO

LITERATURE REVIEW

2.1. Terrestrial Millimeter Wave Propagation

Terrestrial Millimeter wave (mm-wave) outdoor wireless communication systems are primarily deployed in clear line-of-sight environments to avoid high penetration losses due to buildings and foliage. For these communication systems, in order to facilitate planning, installation and post deployment high-quality fiber- like system performance, unfortunately, quantitative analysis of wideband mm-wave propagation channels is difficult to find in literature, particularly at 38 GHz and 60 GHz. This section enumerates primary issues pertaining to microwave propagation in outdoor radio channels and elaborates on diffraction effects. Absorption due to gases and scattering due to precipitation are included in the generalized path loss model. The next section of this thesis presents the literature survey on outdoor propagation measurements performed in the 38 GHz and 60 GHz bands of frequencies. The chief propagation effects that need to be considered in the design of fixed broadband microwave/mm-wave radio link are summarized as follows [ITU]:

- Line-of-Sight (LOS) and Fresnel Zone clearances

- Diffraction due to uneven terrain

- Frequency selective fading due to multipath

- Attenuation and scattering due to vegetation

- Attenuation due to atmospheric gases

- Attenuation and depolarization due to precipitation

These propagation effects can seriously degrade the system performance as a result of reduced system coverage and signal distortion due to frequency selective fading (J.Wait, 1998).

2.2. Transmission Losses

The Friis free-space propagation equation is commonly used to determine the attenuation of a signal due to the spreading of the electromagnetic wave. For frequencies between 500 MHz and 10 GHz, this model provides a good estimate of propagation loss. However, for frequencies above 10 GHz, losses due to molecular resonance and precipitation must be taken into consideration. The total transmission loss for a millimeter link is given by Freeman as: (T.S Rappaport, 1991)

Atten(dB)=92.45+20log10(FGHz)+20log10(Dkm)+TExcess (dB)   **2.1**

TExcess (dB) = a + b + c + d + e   **2.2**

Where,

a = excess attenuation (dB) due to water vapor

b = excess attenuation (dB) due to mist or fog

c = excess attenuation (dB) due to oxygen (O_2)

d = sum of absorption losses (dB) due to other gases

e = excess attenuation (dB) due to rainfall

There are many atmospheric gases and pollutants that have absorption lines in the millimeter bands (such as SO_2, NO_2, O_2, H_2O, and N_2O), however the absorption loss is primarily due to water vapor and oxygen (Sommerfeld, 2000).

2.2.1. Diffraction

Diffraction allows radio signals to propagate around the curved surface of the earth, beyond the horizon, and to propagate behind obstructions. The phenomenon of Diffraction can be explained by Huygen's principle, which states that all points on a wavefront can be regarded as point sources and give rise to secondary wavelets. Combination of all the wavelets produces a new wavefront in the direction of propagation. Fresnel Zones represent successive regions where secondary waves have a path length from the transmitter to receiver which are nλ/2 greater than the total path length of a line-of-sight path. Fresnel zones are elliptical in shape with the transmitting and receiving antenna at their foci, the concentric circles, shown in Fig.2.1,

represent boundaries of successive Fresnel zones. The successive Fresnel zones alternatively provide constructive and destructive interference to the total received signal. The radius of the nth Fresnel zone circle, denoted by r_n, can be expressed by Equation 2.3 (Longley, 200). In Equation 2.3, λ represents the wavelength of the propagating wave and distance parameters d_1 and d_2 are explained in Fig.2.1. The expression is valid for $d_1, d_2 \gg r_n$

$$r_n = \sqrt{n\lambda d1 d2 / d1 + d2}$$
2.3

Diffraction losses occur when the secondary waves are blocked such that only a part of the energy is diffracted around the corner. The total received signal energy is given by the vector summation of energy contributions from all unobstructed Fresnel zones.

Fresnel Zone Boundaries
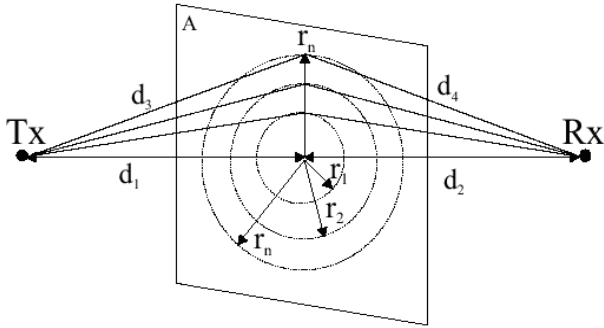
Fig.2.1: Concentric circles that define the boundaries of successive Fresnal zones (li et al, 2000)

Knife-edge Diffraction model is one of the simplest diffraction models that is used to predict losses when diffraction shadowing is caused by a single object such as a hill or mountain. The model is shown in Fig.2.2 and Equations 2.4 and 2.6 express the Fresnel-Kirchoff Diffraction parameter and the Diffraction gain, respectively. It can be shown that the diffraction losses increase with a decrease in the wavelength or increase in the frequency of the propagating electromagnetic wave (Lichun, 2000).

$$\frac{Ed}{E0} = F(v) = \frac{1+j}{2} \int \exp\left(\frac{-j\Pi t^2}{2}\right) dt \qquad\qquad 2.4$$

$$V = h\sqrt{\frac{2(d1+d2)}{\lambda d1 d2}}$$
2.5

G (dB) = 20log $|F (V)|$
2.6

In Equation 2.4, E_d is the electric field strength of the knife-edge diffracted wave while E_0 is the free-space field strength in the absence of ground and knife-edge. Parameters used in Equation 2.5 are explained in Fig.2.2. G_d represents the diffraction gain in Equation 2.6.

Knife-Edge Diffraction
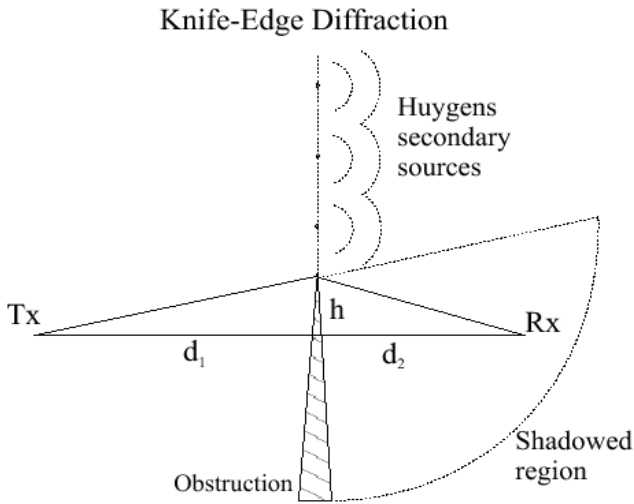
Fig.2.2: Knife-edge Diffraction Model (li et al, 2000)

2.2.2. Scattering: Effects of Vegetation

When a radio wave impinges on a rough surface, the reflected energy is diffused in all directions due to scattering. At millimeter-wave

frequencies, the dimensions of tree leaves, twigs, and tree branches are large as compared to the wavelength. The tree leaves and branches also usually contain water and hence result in absorption and scattering of electromagnetic waves as they propagate through vegetation. Foliage can not only introduce attenuation and broadening of the beam but also depolarization of the electromagnetic wave. The transmission losses through vegetation are affected by various parameters such as the dielectric constant, density, physical size and shape (Longley, 200). International Telecommunications Union (ITU) recommends three different propagation models namely ITU-R, Fitted ITU-R (FITU-R), and the Nonzero Gradient (NZG) model. The ITU-R model was developed from propagation measurements performed at UHF. The transmitter and receivers are positioned such that most of the radio propagation path falls within the vegetation medium. The proposed model is stated to be applicable in the frequency range 200 MHz to 95 GHz. The fitted ITU-R (FITU-R) model attempts to optimize the ITU-R model while the NZG model is a more generalized model based on the maximum attenuation model but without a final fixed slope. For details please refer to (Longley, 2000).The transport theory, referred to as the theory

of radioactive energy transfer, is used to model radio wave propagation

through woods and forests (Felsen and Marcuvitz, 1994).

2.2.3.   Scattering: Effects of Rain

Wireless communication systems operating at frequencies below

10 GHz are least affected by rain. However at millimeter frequencies,

rain induced attenuation (due to absorption and scattering) is one of the

principal factors that increases the overall path loss, limits the coverage

area and consequently degrades the system performance. The ITU

recommends a calculation method for terrestrial systems (King, 1967),

and for satellite to earth links, ITU-R P.618 (Sommerfeld, 2000). The

"Crane" models, after Robert K. Crane, are popular for satellite-earth

links but also have terrestrial models. There are 3 versions of the Crane

models. The Global Crane model was developed in 1980. In 1982 the 2

component Crane model was developed that used a path- integrated

technique. A volume cell contribution and a debris contribution for a

path were computed separately and added to provide a link calculation

(Gibson, 1999). As a refinement of the 2-component model, the revised

two-component model was introduced in 1989 that includes spatial

correlation and statistical variations of rain within a cell. The theoretical

prediction model proposed by Crane, based on the aR^b rain attenuation

model is summarized in Equations 2.7 through 2.12. In these Equations,

A_R is the rain attenuation in dB, R is the point rain rate in mm/hr, and d is

the distance in km. Constants 'a' and 'b' are rain attenuation coefficients

that are functions of frequency and polarization and are tabulated in

(Schmitz and Martin, 2008).

$$A_R = aR^b \left[\frac{\ell^{ubd}-1}{ab} \right] \text{ (for } 0 \leq d \leq D_0\text{)} \qquad\qquad 2.7$$

$$A_R = aR^b \left[\frac{\ell^{ubD_0}-1}{ub} - \frac{B^b\,\ell^{cbD_0}}{cb} + \frac{B^b\,\ell^{cbd}}{cb} \right] \text{(for } D_0 \leq d \leq 22.5\text{km)} \qquad 2.8$$

Where,

$D_0 = 3.8\ 0.6\ \ln(\,R\,)$ 2.9

$B = 2.3R^{-0.17}$ 2.10

$$U = \ln \left[\frac{B^{ecD_0}}{D_0} \right] \qquad\qquad\qquad\qquad\qquad\qquad 2.11$$

$C = 0.026\ =0.03\ln(\,R)$ 2.12

For paths longer than 22.5 km, the attenuation A_R is calculated for

a 22.5 km path, and the resulting rain attenuation is multiplied by a

factor of (d/22.5). Another empirical rain model based on nominal water

droplet sizes and distribution by facilitates calculation of attenuation

rate (dB/km) due to a specified rainfall rate. The model is referred to as

the Simplified Attenuation Model (SAM/ CCIR). The attenuation rate can

be approximately expressed by Equation 2.13, where R represents the rainfall rate in millimeters per hour and parameters 'a' and 'b' are respectively expressed using Equations 2.14 and 2.15.

$K_{rain} = aR^b$ 2.13

$a = 4.21 \times 10^{-5} f^{2.42}$ (for 2.9GHz $\leq f \leq$ 54GHz)   2.14. (a)

$a = 4.09 \times 10^{-2} f^{0.669}$ (for 54GHz $\leq f \leq$ 180GHz)   2.14. (b)

$b = 1.41 f^{-0.0779}$ (for 8.5GHz $\leq f \leq$ 25GHz)   2.15 (a)

$b = 2.63 f^{-0.272}$ (for 25GHz $\leq f \leq$ 164GHz)   2.15. (b)

It is important to note that in Equations 2.14 and 2.15, the frequency f is expressed in GHz (Ajay, 2007).

2.2. Outdoor Propagation Measurements at 38 GHz

Outdoor propagation measurement results, characterizing an urban environment for wideband digital traffic, the measurements are primarily performed over LOS links and reflective properties of urban materials (metal, glass, wet flat roof surfaces etc) are quantified. The study employs a 90-degree transmitting horn antenna and a 20-degree receiving horn antenna to record multipath structure and statistics. Results from a wideband channel sounding program, conducted at 39 GHz and 60 GHz, are summarized and a statistical model for wideband short-range mm-wave channels is presented. Building scatter and

vegetation attenuation measurement results at 38 GHz are elaborated in (Vaughan et al, 2003).The results from CW measurements of specular and non-specular reflections of one face of a 2-storey building indicate that contribution from cross-polar reflections is generally lower than from co-polar non-specular reflection. Cross-polar effects are therefore less significant from the point of view of interference prediction. The attenuation measurements were performed through dense sycamore and lime trees with vegetation depths ranging from 0 to 46m. A standard gain pyramidal horn antenna was used as transmitter and receiver antenna heights were chosen as 3m, 5m and 7m from the ground level to facilitate propagation measurements at trunk level, foliage level and treetop level, respectively. Measured results indicate that signal attenuation due to vegetation varies with height and is minimal at the trunk level. Propagation results also indicate that signal attenuation increases sharply over shorter vegetation depths. However, as the vegetation depth increases, scattering from trees tends to contribute towards the received signal and hence the increase in signal attenuation is not as sharp. The thesis also compares the measured attenuation statistics with the ITU recommended model and proposes

an improved semi-empirical model based on the measured data at 38 GHz (Longley, 2000).

Mazanek discusses depolarization caused by raindrops over a propagation link length of 52 m. The transmitting and receiving antennas are placed 32 m above the terrain throughout the propagation study. Theoretical attenuation for the vertical and horizontal polarization is shown as a function of the rain-rate at 37 GHz. Wideband measurement campaigns are performed at 38 GHz on three point-to-point links, including a 605 m LOS link, a 265 m partially obstructed link and a 265 m link obstructed by vegetation. The results from propagation measurement campaigns, performed during clear sky, moderate to heavy rain and hail conditions, indicate that time dispersion characteristics of a radio channel may change during different weather events. In the study, fewer numbers of multipath components were detected during clear sky conditions than during moderate to heavy rain conditions. The results also show that received signal variation during rain follows a Rician distribution. In the thesis, the rain attenuation statistics calculated from measured propagation data are compared with the Crane model. Upper and lower bounds for the Crane model are presented based on the measured rain attenuation data. The theoretical

study, based on fundamental principles of wave propagation through random media of scatters, also shows that non-uniform distribution of raindrop density along the propagation path can result in signal fluctuation (Backman, 2003).

2.3. Outdoor Propagation Measurements at 60 GHz

Electromagnetic wave propagation at 60 GHz band of frequencies experiences much higher path loss due to diffraction, scattering due to vegetation, scattering due to rain and oxygen absorption. Two propagation models for average path loss estimation and received power calculation at millimeter wave frequencies, specifically 60 GHz (Saunders, 2000). The report also includes recorded impulse responses and results from propagation measurements performed in an urban street environment at 60 GHz. The results, from measurements over radio link lengths of 30 - 160 m, indicate that received power fluctuates by as much as 4 - 8 dB for LOS links due to multipath frequency selectivity and 6 - 8 dB for LOS links partially obstructed by trees (Medeisis and Kajackas, 2000).

2.4. Free Space Path-loss for LOS Environment

Free space path loss provides a means to predict the received signal power when there is no object obstructing the LOS path between

the TX and the RX. The model for path loss in a LOS environment is straightforward. The received power Pr is related to the transmitted power Pt via the Friis transmission formula (Rappaport, 2002):

$$P_r = \frac{EIRP}{4\pi d^2} A_e = \frac{P_t G_t G_r \lambda^2}{(4\pi d)^2}$$ 2.16

In (2.16), $EIRP = P_t G_t$. The transmitting antenna has gain G_t while the receiving antenna has gain G_r. Distance d is the separation between the TX and the RX. The RX has an effective aperture given by $A_e = \frac{G_r \lambda^2}{4\pi}$ where λ is the signal wavelength. The path loss is defined by the term

$$L = \frac{P_r}{P_t G_t G_r} = \frac{A_e}{4\pi G_r d^2} = \left(\frac{\lambda}{4\pi d}\right)^2$$ 2.17

It is shown that for the LOS environment, the power received will fall off with the square of the distance between the TX and the RX.

2.5. Path-loss for NLOS Environment

Since there are scattering objects in the channel, it is quite likely that the transmitted signal cannot reach the RX directly since the LOS path is blocked by these objects. These objects can greatly impact the average signal strength at the RX.

Unlike the LOS case, the modeling of path loss in the NLOS environment is more complex and involves more environmental parameters in the

model. A popular NLOS path-loss model is semi empirical and assumes

the form (Andrea, 2005):

$$L(d) = P_L(dO) + 10n \, log_{10}\left(\frac{d}{do}\right) + S_{(d)} [dB] \qquad 2.18$$

$PL(d_0)$ is the path loss at a reference distance d_0 from the TX, $S_{(d)}$

accounts for the lognormal shadow fading effects, and n is the path-loss

exponent. Many experiments and results have been reported for both

LOS and NLOS environments, covering the frequency range from 100

MHz to 2 GHz, which is the frequency band for most narrowband

transmission systems. According to (2.18), path-loss is assumed to be the

linear function of log distance (to the base 10) with loss exponent n and

intercept $PL(d_0)$.These loss exponents and intercept values are subject

to change for different environments and generally do not equal to the

values for LOS environment. Normally the loss exponents and intercept

values are typically determined by taking several measurements at

various distances and performing a linear regression to obtain a least

square fit to the measured data (Erceg et al, 1999).

2.6. Semi-empirical Path-loss Models for Macro-cell Areas

There are numerous semi-empirical models in the literature aiming to

predict the path loss over different environments. The models

demonstrated below are models derived from measured data corresponding to macro cellular environments with path distances ranging from 1 km to over 10km. The Hata and Lee models are the most commonly used models for signal prediction in urban areas nowadays although they were developed long ago. Many telecommunication providers are using these models in designing and optimizing their radio networks. The common characteristic of all the models is the linear dependence of path-loss on the distance from the TX to the RX, as depicted in (2.18). Various path loss exponents and intercept values are reported in these models with respect to different environments. Two typical models: the Hata model, the Lee model, which are best suitable for urban areas (Longley, 200).

2.6.1. Okumura Model

The Okumura model is applied when frequencies range from 150 KHz to 1920 MHz and distances from the TX to the RX, range from 1 km up to 100 km. The model is based on measured data taken in Japan. This is among the simplest models and becomes the standard for path-loss modeling. The standard deviation in predicting the path loss is around 10 dB. The model is described by

$$L \ (dB) = LF + Amu \ (f \ ,d) - G(ht \ ) - G(hr \ ) - G_{AREA} \qquad (2.19)$$

where $L(dB)$ is the median path loss, LF is the free space path loss calculated by (2.17), Amu (f, d), the median loss relative to free space, is a set of curves developed from measured data using omni-directional antennas, $G(ht)$ is the base station (BS) gain factor with height ht, $G(hr)$ is the MS gain factor with height hr, and $GAREA$ is the environment gain factor (Medeisis and Kajackas, 2000). These gain factors are given by

$$G_{(ht)} = 20\log_{10}\left[\frac{ht}{200}\right], \quad 1000m > ht > 30m \qquad 2.20$$

$$G_{(ht)} = \left\{ \begin{array}{l} 20\log_{10}\left(\frac{h_r}{3}\right), \ h_r \leq 3m \\[2mm] 20\log_{10}\left(\frac{h_r}{3}\right), \ 10m > h_r > 3m \end{array} \right. \qquad 2.21$$

The median loss Amu (f,d) and the environment gain factor G_{AREA} are available as Okumura curves shown in Fig.2.3 and 2.4.

2.6.2. Hata Model

Hata further developed the Okumura model from the semi-empirical path loss data provided by Okumura. The Hata model is mostly applicable for urban areas that have not been addressed in the Okumura model. The model is best accurate within a frequency range from 150 KHz to 1500 MHz.

The basic formula for the median path loss $L(dB)$ given by Hata is

$L(dB)=69.55+26.16\log fMHz-13.82\log ht-a(hr)+(44.9-6.55\log ht)\log dkm$ (2.22)

Where ht and hr are base station and mobile station antenna heights in meters, respectively, dkm is the link distance or cell radius in kilometers, $fMHz$ is the centre frequency in megahertz, and the 10 terms $a(hr)$ and K are vehicular station antenna height-gain correction factor and environment correction factor, respectively, which depend upon the environment (Hata, 1999). These correction factors for different environments are tabulated in Tables 2.1 and 2.2 below.

Table 2.1: Urban Environment Correction Factors for Hata Model (Hata, 1999).

Environment type	K	a(hr)
Urban indoor large city	0	$8.29(\log 1.54hr)^2 - 1.1-15.0$, $f_{MHz}<200mHz$. $3.2(\log11.75hr)^2 -4.97 -15.0$ $f_{mHz} > 400MHz$
Urban large city	0	$8.29(\log1.54hr)^2 - 1.1$, $f_{MHz} < 200MHz$ $3.2(\log11.75hr)^2 -4.97$, $f_{mHz} > 400MHz$
Urban small city	0	$(1.11\log f_{MHz} - 0.7)hr - (1.56\log f_{MHz}-0.8)$.

Table 2.2: Sub-Urban and Rural Environment Corrections Factors for Hata

Model (Hata, 1999)**.**

Environment type	K	A(hr)
Sub urban	$$2\left[\log\left(\frac{fmHZ}{28}\right)\right]^2 + 5.4$$	0
Rural indoor (quasi-open)	4.78(logFmHZ)^2 18.331 logFmHZ + 35.94-10	0
Rural (quasi-open country side)	4.78 (logFmHZ)^2 -18.331logFmHZ+35.94	0
Rural (open)	4.79(logFmHZ)^2 – 18.331/ogFmHZ + 40.94	0
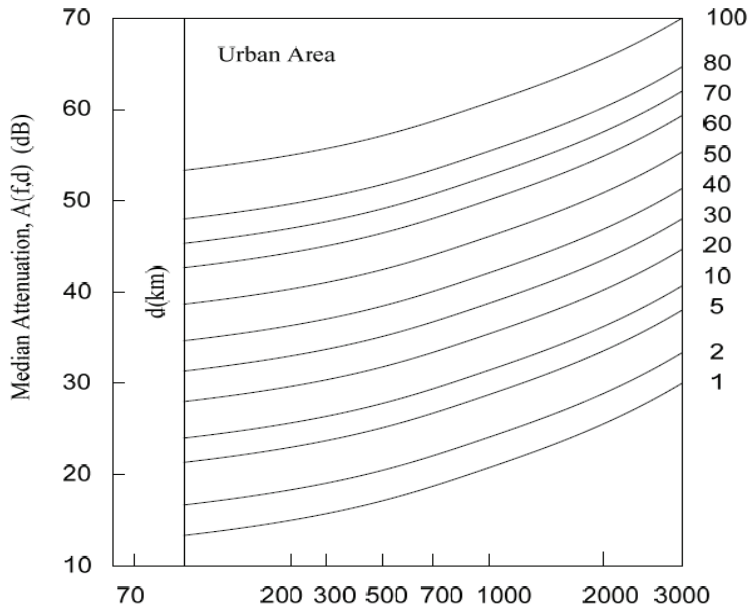
Fig. 2.3: Median Loss Relative to Free Space A_{mu} (f,d) (Hata, 1999)
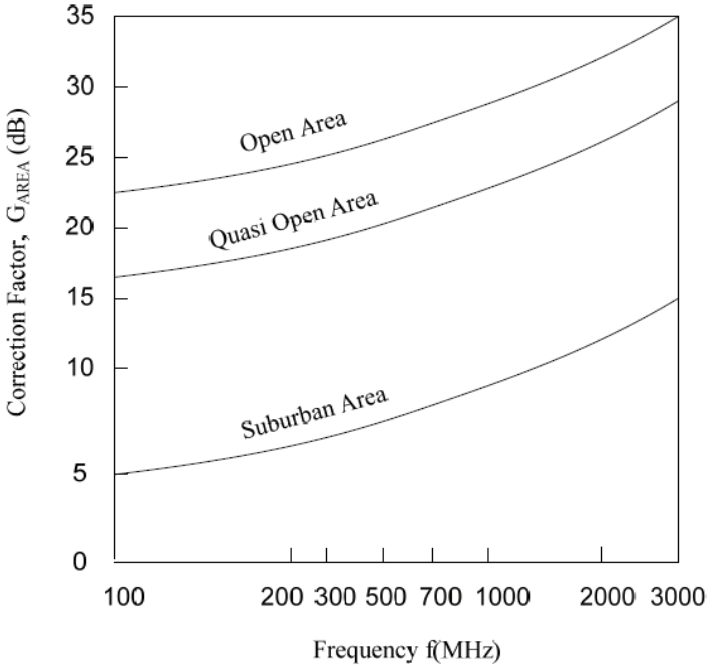
Fig. 2.4: Correction Factor for Different Environments (Longley, 200).

2.6.3. COST-231 Model

COST-231 model is the extended version of the Hata model developed by EURO-COST. This model extends the Hata model's frequency range from 150 KHz to 2000 MHz. The model has a slight difference in the intercept value but the same exponent compared with the Hata model. The model's path loss is given by

$L(dB) = 46.3 + 33.9 \log f_{MHz} - 13.82 \log h_t - a(h_r) + (44.9 - 6.55 \log h_t) \log d_{km} + C_M$ (2.23)

Where

$C_M= \begin{cases} 0dB \\ 3dB \end{cases}$ (for medium sized city and suburban areas, for metropolitan

centers)

In (2.23), $a(hr)$ is the same as in Hata model and is defined in Tables (2.1)

and (2.2), ht and hr are also base station and mobile station antenna

heights in meters, respectively, dkm is the link distance or cell radius in

kilometers, and $fMHz$ is the centre frequency in megahertz. Both the

Hata and COST-231 models restrict the above parameters in the

following ranges (Rappaport, 1991)

h_t :1km 20km

h_r :1m 10m

d :30m 200m [61].

2.6.4. Lee's Model

Lee's model is applicable only to flat areas; otherwise significant

prediction errors may be introduced. The model is specified as follows:

$$Pr = 10log_{10}\left[P_0 \left(\frac{d}{do}\right)^{-n} \left(f/fo\right)^{-\beta} \alpha_o\right]$$ 2.24

In (2.24), P_r , P_0 , f , and f_0 are, respectively, the received signal power at

distance d from the TX, the received signal power at reference distance

d_0 (typically 1.6 km), the carrier frequency, and the nominal carrier

frequency (typically 900 MHz). The path loss exponent n is empirically derived and location-dependent. The exponent β varies with the carrier frequency. The correction factor α_0 accounts for the antenna heights, the transmit power, and the antenna gains (Sharma et al, 2011). The correction factor α_0 is calculated with the frequencies greater than 30 MHz as below.

$$\alpha_0 = \alpha_1\alpha_2\alpha_3\alpha_4\alpha_5 \tag{2.25}$$

Where:

$$\alpha_1 = \left(\frac{BS\ antenna\ height(m)}{30.48cm}\right)^2 \tag{2.26}$$

$$\alpha_2 = \left(\frac{MS\ antenna\ height(m)}{3(m)}\right)^V \tag{2.27}$$

$$\alpha_3 = \left(\frac{Transmit\ Power\ (w)}{10(w)}\right)^W \tag{2.28}$$

$$\alpha_4 = \left(\frac{BS\ antenna\ gain\ with\ respect\ to\ half\ wavelenght\ dipole}{4}\right) \tag{2.29}$$

α_5 = different antenna gain correction factor at MS

The variable v in α_2 equals 2 when the MS antenna height is greater than 10 m and equals 1 when MS antenna height is smaller than 3 m.

For convenience, the path-loss models for different environments proposed by Lee are summarized as follows:

$$L(dB) = X + Y \log_{10}(dB) + 10m \log_{10}\left(\frac{f}{f_0}\right) - \alpha_0 (dB)$$　　　2.30

Table 2.3: Environment Parameters for Lee Model (Sharma et al, 2011)

Type of emission	X	Y
Free space	96.92	20.0
Open area	86.12	43.5

2.6.5.　ECC-33Model

The ECC-33 model is developed by Electronic communication committee (ECC). This is generally used for FWA (Fixed Wireless Access) system. The path loss is defined as (Armoogum et al, 2007).

PL (dB) = A_{fs} + A_{bm} − G_b − G_r　　　*2.31*

Where,

A_{fs}, A_{bm}, G_b and G_r are the free space attenuation, the basic median path loss, the BS height gain factor and the terminal height gain factor. They are the individually defined as,

A_{fs} = 92.4 + 20 log10(*D*) + 20 log10(*f*)　　　2.32

A_{bm} = 20.41+9.83log10(*D*)+7.894log10(*f*)+9.56[log10(*f*)]^2　　　2.33

G_b=log10 (h$_b$/200){13.958+ 5.8[log10(D)]^2}　　　2.34

And for medium city environments,

G_r= [42.57+13.7log10 (*f*)][log10(h$_r$) − 0.585]　　　2.35

Where

f is the frequency in GHz, D is the distance between Transmitter and Receiver in km, h_b is the BS antenna height in meters and h_r is the CPE antenna height in meters. The predictions using the ECC- 33 model with the medium city option are compared with the measurements taken in suburban and urban environments (Sharma, 2010).

2.6.6.   Stanford University Interim (SUI) Model

The proposed standards for the frequency bands below 11 GHz contain the channel models developed by Stanford University, namely the SUI models. Note that these models are defined for the Multipoint Microwave Distribution System (MMDS) frequency band in the USA, which is from 2.5 GHz to 2.7 GHz. Their applicability to the 3.5 GHz frequency band that is in use in the UK has so far not been clearly established (Ayyappan and Dananjayan, 2007). The SUI models are considered into three types of terrains, namely A, B and C. Type A is associated with maximum path loss and is appropriate for hilly terrain with moderate to heavy foliage densities. Type C is associated with minimum path loss and applies to flat terrain with light tree densities. Type B is characterized with either mostly flat terrains with moderate to heavy tree densities or hilly terrains with light tree densities. The basic

path loss equation with correction factors is presented by (Erceg et al, 1999).

$$PL = A + 10\gamma \log 10 \, d/d_0 + X_f + X_h + s \text{ for } d > d_0 \qquad 2.36$$

where, d is the distance between the AP and the CPE antennas in meters, $d_0 = 100$ m and s is a log normally distributed factor that is used to account for the shadow fading owing to trees and other clutter and has a value between 8.2dB and 10.6dB. The other parameters are defined as,

$$A = 20 \log 10 \, (4\pi d_0 / \lambda) \qquad 2.37$$

$$\gamma = a - b h_b + c/h_b \qquad 2.38$$

Where,

The parameter h_b is the base station height above ground in meters and should be between 10m and 80m. The constants used for a, b and c are given in Table 2.4. The parameter γ is equal to the path loss exponent. For a given terrain type the path loss exponent is determined by h_b.

Table 2.4: Numerical Values for the SUI Model (*IRE, 1997*).

Model parameters	Terrain A	B	C
A	4.6	4.0	3.6
B(m^{-1})	0.0075	0.0065	0.005
c(m)	12.6	17.1	20

The correction factors for the operating frequency and for the CPE antenna height for the model are,

X_f = 6.0 log10 (f/2000)   2.39

X_h = −10.8log10 (h$_r$/2000), for terrain types A& B   2.40

   = −20.0log10 (h$_r$/2000), for Terrain type C   2.41

Where *f* is the frequency in MHz and *h$_r$* is the CPE antenna height above ground in meters. The SUI model is used to predict the path loss in all three environments namely rural, suburban and urban.

2.6.7.   Egly Propagation Model

Egly is simplified model that assumes gently rolling terrain with average hill heights of approximately 50 feet, because of this assumption, no terrain elevation data between the transmit and receive facilities is needed. Instead, the free space propagation loss is adjusted for the height of the transmitter and receiver antennas above ground. As with many other propagation models, Egli is based on measured propagation paths and then reduced to mathematical model. In case of

Egli, the model consists of a single equation for the propagation loss (Srinivasa and Haenggi, 2007).

$$A = 117 + 40\log D_{mile} + 20\log F - 20\log (H_T * H_R) \qquad 2.42$$

Where:

A is the attenuation in dB (between dipole)

D is the path distance in miles

F is the frequency in Mega Hertz

H_T is the transmitter antenna height above ground level (AGL) in feet

H_R is the receiver antenna height above ground level in feet

The typical equation used for Free Space loss between half wave dipole antennas (in dB) is

$$A_{FS} = 32.27 + 20\log D_{miles} + 20\log_{FMHZ} \qquad 2.43$$

To isolate the propagation of the loss attributable to Egli consideration, subtract the free-space portion from the computed Egli attenuation:

$$A_{FS} = 84.73 + 20\log D_{miles} 20\log(H_T * H_R) \qquad 2.44$$

If the value of A Egli is zero or less, then free space valued is used. The Egli model should not be used in such type of areas like areas of rugged terrain, significant obstructions etc. Egli says it is limited to those areas which are similar to plain earth, such as relatively short over water and very flat barren land paths.

2.7. Performance Analysis

2.7.1. Path Loss Calculation

Path loss is derived by the Transmission path from a base trans receiver station to the mobile station is shown by as

$$PL(db) = P_{TX} + G_{TX} - L_{TX} - P_{RX} - L_{RX} - L_M \qquad 2.45$$

P_{TX} = Transmitted Output power

G_{TX} = Transmitter antenna Gain(db)

L_{TX} = Transmitter Losses (db)

P_{RX} = Received Power (dbm)

L_M = miscellaneous losses (db)

The difference between the measured path loss and the predicted path loss is known as Error. The relative error is defined as

$$\text{Relative Error} = \frac{PL(measured) - PL(predicted)}{PL(measured)} \qquad 2.46$$

The Relative error and Path loss exponent shows how much path loss between the transmitter and receiver and the Table 2.6 shows the Error and path loss exponent for different models.

Table 2.5: Error And Path Loss Exponent For Different Environment (Ozg, 2007**).**

Path loss model	Relative Error	PLE
Hata-Okumara	0.39	3.44
ECC-33	0.43	3.71
Egli	0.48	4.00
SUI	0.50	4.16
Cost-231	0.41	3.45

2.8 Path Loss Exponent Estimation

This section describes three completely distributed algorithms for PLE estimation; each based on a certain network characteristic, and provides simulation results on the estimation errors. The first algorithm uses the mean value of the interference and assumes that the network density is known beforehand. Algorithms 2 and 3 are based on outage probabilities and the network's connectivity properties respectively, and do not require knowledge of λ or the Nakagami parameter m. The PLE estimation problem is essentially tackled by equating the empirically (observed) measured values of the aforementioned network characteristics to the theoretically established ones to obtain γ. In each time slot, nodes either transmit (w.p.p) or listen to record measurements (w.p.1–p). Upon obtaining the required measurement values over several time slots, the estimation process can be performed at each node in the network in a distributed fashion. The PPP is

generated by distributing a Poisson number of points uniformly

randomly in a 50 × 50 square with density 1. To avoid border effects, we

use the measurements recorded at the node lying closest to the center

of the network. To analyze the mean error performance of the

algorithms, we consider the estimates resulting from 50, 000 different

realizations of the PPP. The contention probability is taken to be p = 0.05

in each case2, and N_0 = −25dBm.

2.8.1. Algorithm 1: Estimation Using the Mean Interference

In many situations, the network density is a design parameter and

known. In other cases, it is possible to estimate the density. A simple

technique to infer the PLE when the nodal density is known is based on

the mean interference in the network. According to this method, nodes

simply need to record the strength of the received power that they

observe and use it to estimate. For > 2 (a fair assumption in a wireless

scenario), the mean interference is theoretically equal to (Ozg, 2007).

$$C_n = 2\pi\lambda_p E_G\left[G^m\right]\frac{B^{2-n\gamma}-A^{2-n\gamma}}{2-n\gamma}$$ 2.47

In particular, we can consider only the case > 2 (a fair assumption in a

wireless scenario) and let B be large (considering the entire network) so

that the mean interference is

$$u_1 = c_1 = 2\pi\lambda_p \frac{A^{2-\gamma}}{2-\gamma} \qquad\qquad 2.48$$

Which is independent of m consequently, the mean received power is

$\mu_R = \mu_I + N_0$. Note that the mean received power is infinite for A = 0.

However, the large-scale path loss model is valid only in the far-field of

the antenna and breaks down for very small distances. Denote the

(known) near-field radius by a positive constant A_0. The algorithm based

on the mean interference matches the sample and theoretic values of

the mean received power and are described as follows.

• Record the strengths of the received powers $R_1, \ldots R_N$ at any

arbitrarily chosen node during N time slots. Eventually, the empirical

mean received power $(1/N)\sum_{i=1}^{N} R_i$ converges.

• Equate the empirical mean to the theoretical value of μ_R (with $A=A_0$)

and estimated γ using a look-up table and the known values of p, N_0, A_0

and estimated (known or estimated density). Fig. 2.5 depicts the mean

squared error (MSE) values of the estimated PLE γ using the above

algorithm for different γ and N values. The estimates are seen to be

fairly accurate over a wide range of PLE values.

2.8.2. Algorithm 2: Estimation Based on Virtual Outage Probabilities

We now describe an estimation method based on outage probabilities that does not require the knowledge of the network density or the Nakagami fading parameter. We first overview some theoretical results and then present a practical scheme to estimate, It is shown that when the signal power is exponentially distributed, the success probability p_s across any link in the Poisson network is equal to the product of the Laplace transforms of noise and interference. In particular, when the transceiver pair separation is unity, we have (Stoyan, 2002).

$$P_s \approx exp\left(-C_1 \theta^2 / \gamma\right) \qquad 2.49$$

To estimate γ, the nodes are required to measure the SIR values during several time slots and use it to compute the empirical success probability, which matches the theoretical value. However, note that it is impractical to place transmitters for each receiver node where a SIR measurement is taken. Instead, nodes can simply measure the received powers, and compute the (virtual) SIRs taking the signal powers to be independent realizations of an exponential random variable.

This algorithm is implemented at each node as follows.

• Record the values of the received powers $R_1, \ldots R_N$ at the node during N time slots. Take the signal powers S_i, $1 \le i \le N$, to be N independent realizations of an exponential random variable with unit mean. Using the values S_i/R_i $\forall i$, a histogram of the observed SIR values is obtained.

• Evaluate the empirical success probabilities at two different thresholds, i.e., compute $p_{s,j} = (1/N)\sum_{i=1}^{N} 1\,[S_i/R_i > j = 1, 2]$. Eventually, the success probability values converge.

• match the empirically observed values.

$$\bar{\gamma} = \frac{2ln(\theta_1 \theta_2)}{\ln(\ln(P_{Sj})/lnP_{S2})} \qquad\qquad 2.50$$

Fig.2.6 plots the MSE of γ for θ_1 = 10 dB and θ_2 = 0 dB for different and N values. We observe that the error is small when the PLE is small, but increases with larger values of. Also, Fig.2.7 plots the MSE of γ versus m at various PLE values for the estimation method based on outage probabilities. We observe that the algorithm performs more accurately at lower values of m.

2.8.3. Algorithm 3: Estimation Based on the Cardinality of the Transmitting Set

When the network density Λ or the Nakagami parameter m, the PLE can be accurately estimated based on the connectivity properties of the network. In this subsection, we derive the average number of nodes

that are connected to any arbitrary node in the network, and describe a PLE estimation algorithm based on our analysis. For any node, define its *transmitting set T(y)* as the group of transmitting nodes whom it receives a (correctly decodable) packet from, in a given time slot. More formally, for receiver y, transmitter node x is in its transmitting set if they are connected, i.e., the SINR at y is greater than a certain threshold θ. Note that this set changes from time slot to time slot. Also note that for $\theta = 0$ dB, the condition for a transceiver pair to be connected is that the received signal strength is greater than the interference power. Thus, for $\theta \geq 1$, the cardinality of the transmitting set, $|T(y)|$, can at most be one, and that transmitter is the one with the best channel to the receiver. The estimation algorithm is based on matching the theoretical and empirical values of the mean number of elements in the transmitting set.
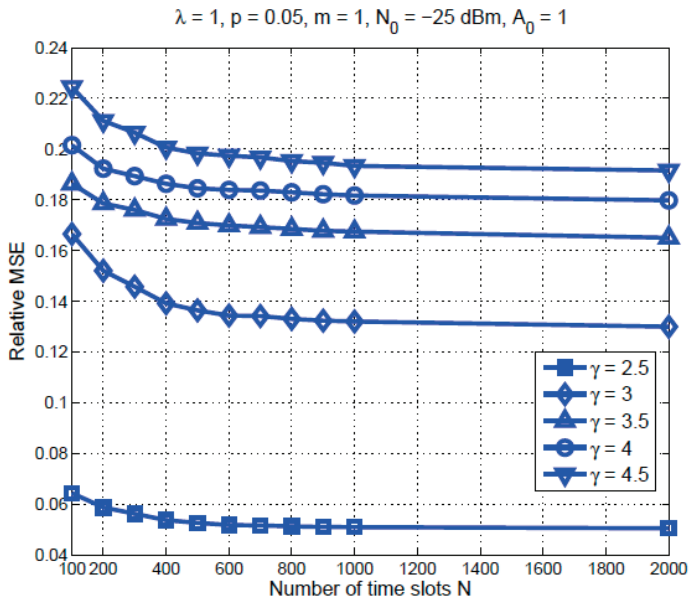
Fig.2.5: Relative MSE of versus the number of time slots for different PLE values, for the estimation method based on the mean interference. The error is small, in particular when the PLE is small (Longley, 2000).
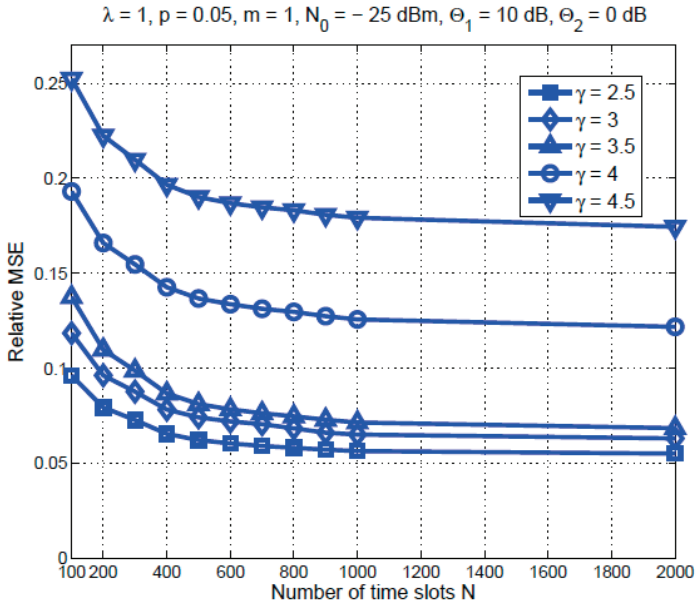
Fig.2.6: MSE of γ versus the number of time slots for the estimation method based on virtual outage probabilities (Longley, 2000).
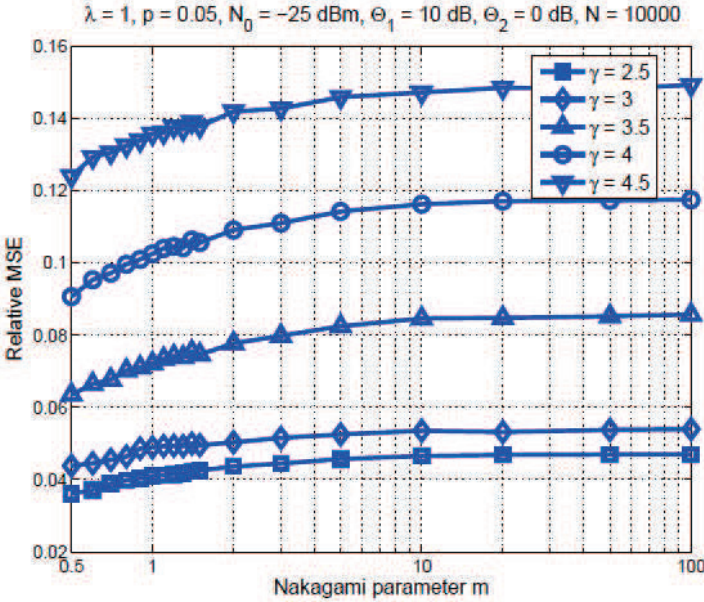
Fig.2.7: MSE of γ versus the Nakagami parameter m for different PLE values, for the estimation method based on virtual outage probabilities (Longley, 2000).

2.9. Improving the Estimation Accuracy

As mentioned, the values measured at the nodes match the theoretical values more closely if each node has access to a larger number of realizations of the process. Fortunately, in the scenario where nodes are distributed as a homogeneous PPP, we can employ two simple ways based on this principle to improve the estimation accuracy. We describe them in this section and also provide simulation results on the

MSE that validate the significant improvement in the performance of the estimation algorithms.

2.9.1. Mobile Nodes

Assume that nodes are mobile and that in each time slot, they each move with a constant velocity v in a randomly chosen direction θ that is uniformly distributed in [0, 2π) (random waypoint mobility model). Since the nodes move independently, each node observes a different PPP realization (with the same density) in each different time slot. By recording measurements over different time slots, can be estimated more accurately. Fig.2.8 plots the relative MSE of γ for each of the three methods when v = 0.115 m/slot. The dashed lines represent the relative MSE when mobility is not considered, and are also plotted to depict the improvement in performance (Zhao et al, 2004).

2.9.2. Coordinating Nodes

Alternatively, if nodes in a neighborhood can coordinate and exchange information, then their measurements can be combined to yield a more accurate estimate of the PLE. Since the homogeneous PPP is ergodic, its statistical average (obtained over different PPP realizations), and its spatial average (obtained over different nodes in a single realization) are equal almost everywhere in the limit (Rappaport,

2002). Based on this result, the estimation process can be performed more accurately on a single realization of the network by collecting the recorded measurements over several nodes.

Fig.2.9 plots the relative MSE of the estimate versus the number of coordinating nodes K. From the figure, we see that the MSE sharply reduces with larger K. As mentioned earlier, with K → 1, the relative MSE → 0.

2.10. SENSITIVITY OF THE ALGORITHMS

We have formalized our algorithms based on the homogeneous PPP model and a spatially invariant path loss assumption. However, in reality, it is more likely that the nodal arrangement is not completely spatially random but takes on other forms such as being clustered or more regular. Also, the PLE value changes depending on the terrain type and the environmental conditions and hence cannot always be taken to be a constant over the entire network. In this section, we briefly comment on the sensitivity of our algorithms to these issues and illustrate how the PLE may be accurately estimated well even when some assumptions are relaxed.

2.10.1: Spatial Invariance of the PLE

In this subsection, we address the case where the PLE is not spatially invariant. For illustration purposes, we consider part of a network consisting of a square subregion A of side l centered at the origin with PLE 1, and an outer region B of PLE 2 as shown in Fig.2.10. To model the path loss, we use the multi-slope 16 piecewise linear model (Longley, 200).Accordingly, for transmitter node n_1 and receiver node n_2, the path loss over a distance r_1+r_2 (see Fig.2.10) is $(r_1/r_0)^{-\gamma_1}.(1+r_2/r_1)^{-\gamma_2}$, for $r_1 > r_0$, where r_0 is the near-field radius. Under this setting, we study the error performance of Algorithm 3 for different locations along the x-axis. Fig.2.11 plots the relative MSE of γ when l = 10 with γ_1 = 4 and γ_2 = 3 and shows that Algorithm 3, by itself, works quite accurately even in a network with two different values of γ. The same qualitative behavior can be expected from Algorithms 1 and 2. For cases where the PLE varies more rapidly or when the network is sparse, nodes can coordinate to obtain better estimates. To accurately do this, it is helpful if nodes have a general idea of the *PLE coherence length*, i.e., the distance over which the PLE can be assumed to be invariant. This may vary from about a mile if the network terrain changes rapidly to as much as hundreds of miles if the network extend from an urban to a suburban to a rural area. It can

be assumed that the network operator has a general idea about variations in the PLE and based on this, the network is divided into sub-areas with constant PLEs, each of which is estimated separately. For instance, if the PLE coherence length is d, each node can estimate the PLE based on measurements recorded by other nodes that lie inside a disk of radius d around it.
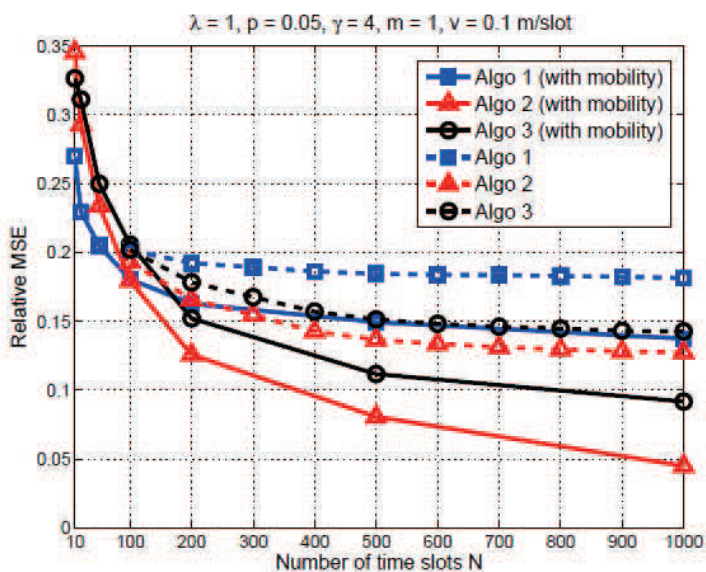
Fig.2.8: Relative MSE of versus the number of time slots, for the three estimation algorithms, with and without consideration of mobility (Longley, 2000).
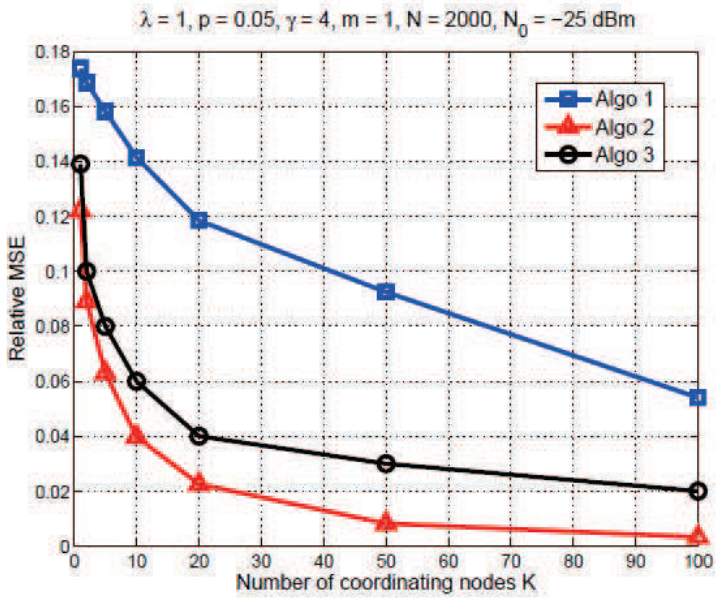
Fig.2.9: Relative MSE of versus the number of coordinating nodes, for each of the estimation algorithms (Longley, 2000).
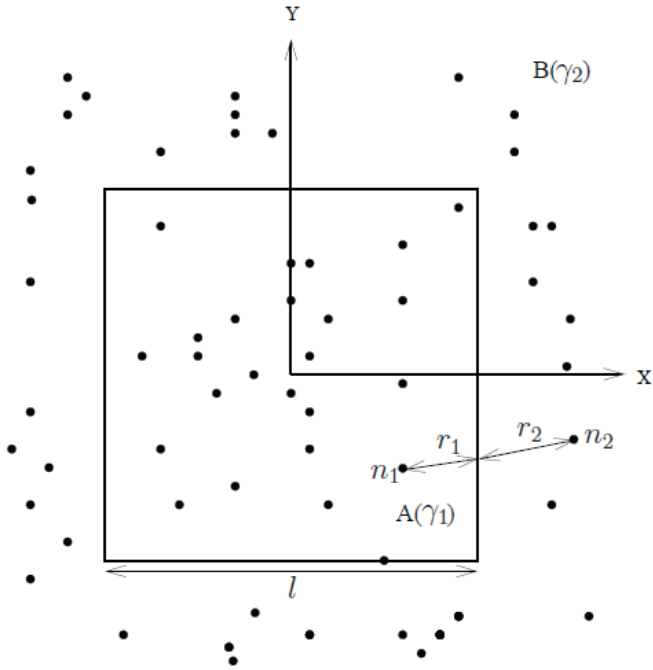
Fig.2.10: The considered Poisson network model with the square sub region A having a different value of PLE, compared to the rest of the network B. The attenuation between nodes n_1 and n_2 is modeled by a piecewise linear path loss model (Longley, 2000).

$\lambda = 1, p = 0.05, m = 1, N_0 = -25 \text{ dBm}, \Theta_1 = 10 \text{ dB}, \Theta_2 = 0 \text{ dB}, l = 10, N = 2000$
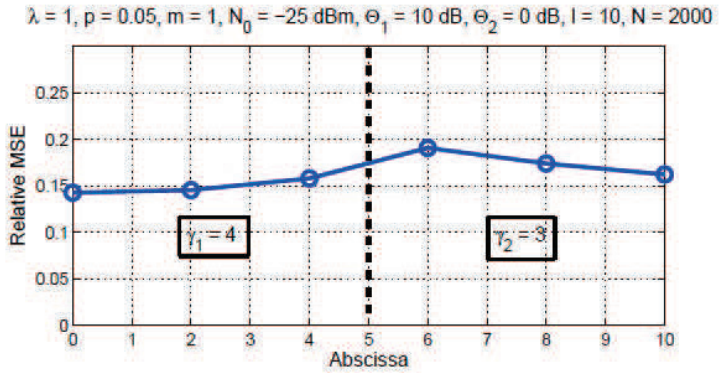
Fig.2.11: Relative MSE for algorithm 3 at different locations (x, 0). The true values of the PLE are $y_1 = 4$ for $x \leq 5$ and $y_2 = 3$ for $x > 5$ (Longley, 2000).

2.10.2. Other Point Process Models

Even though all the algorithms are formulated for the case of the homogeneous PPP, they may also be used to estimate the PLE in different spatial point process patterns. The idea is to artificially make the arrangement of nodes appear more "spatially random". This can be effectively performed upon simply employing randomized power control, wherein instead of having all the nodes transmit at unit power, we let nodes transmit at power levels drawn from a certain distribution. In fact, with independent thinning and appropriate rescaling, every point process is transformed into a stationary PPP (in the limit p → 0). A good

choice for the distribution of transmit power levels is the exponential distribution since it is also the maximum non-negative entropy distribution (Stoyan et al, 2000) i.e., among all continuous pdfs supported on $[0, \infty)$ with a given mean, the exponential distribution has the maximum entropy. Upon employing power control, the algorithms designed for the PPP case may also be used to estimate the PLE for other point processes. Fig.2.12 plots the relative MSE values for Algorithm 3 for three non-PPP network models: the regular lattice grid, the Matern hard core process and the Thomas cluster process (for details on these point processes (Turkmani et al, 2000)), and shows that the algorithm's performance is quite accurate when power control (based on the exponential distribution) is employed. Similar qualitative behavior may be expected of Algorithms 2 and 3. Using power control improves the estimation accuracy even in the case that the nodal arrangement is a PPP since it helps realize diverse realizations of the PPP.
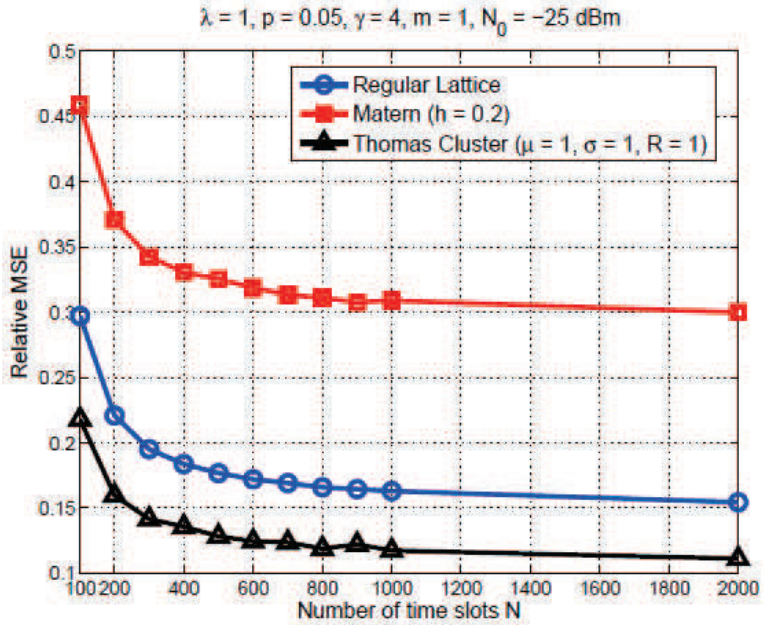
Fig.2.12: Relative MSE of versus the number of time slots, for three non-

PPP models. In each case, Algorithm 3 is found to estimate accurately

(Longley, 2000).

CHAPTER THREE

METHODOLOGY

3.1. Introduction

This section presents the measurement, readings of signal levels in different locations in Ekpoma, Edo State Nigeria. The locations included Ujoelen Ekpoma, Egaure Ekpoma, Emaudo campus, A.A.U. Ekpoma and college of medicine campus, A.A.U. Ekpoma. Signal from MTN service provider was measured. The network operators and their operating frequencies are shown in Table 3.1.

Table 3.1: Network Operators and Their Frequency Bands

Network Operators	Frequency Band	
	900 MHZ	1800 MHZ
Glo	Downlink (945 - 950) Uplink (900 - 905)	1820 - 1835
MTN	Downlink (950 - 955) Uplink (905 - 910)	1835 - 1850
Zain	Downlink (955 - 960) Uplink (910 - 915)	1850 - 1865

For the purpose of this thesis, MTN network provider was considered and frequency band of 1800 MHZ was also considered. (Clint and Daniel, 2000).

The approach taken in the process of doing this work was to measure the signal strength in decibel-meter (dBm) and the corresponding distance to site in kilometer of the chosen locations and the geographical locations and their description are given in Table 3.2:

Table 3.2: Description of Locations

Name of location	Type of location	GPS/location	Description
Ujoelen U_1	Beginning of Ujoelen	Mobile latitude 6^0 44'27.89" Mobile longitude $6^0$7'28.191" GPS accuracy ± 16.om.	Theology bible School at ujoelem extension was taken as the beginning.
Ujoelen U_2	Ending of Ujoelen	Mobile latitude 6^0 44' 38. 968" Mobile longitude $6^0$7'10.947 GPS Accuracy ± 16.0m.	Alli square round – about was taken as the ending of Ujoelen
Eguare E_1	Beginning of Eguare	Mobile latitude 6^0 44' 32.691" Mobile latitude $6^0$7'23.629 GPS Accuracy ± 8.0 ft.	Market square was taken as the beginning of eguare
Eguare E_2	Ending of Eguare	Mobile latitude 6^0 44' 35.398" Mobile latitude $6^0$8'48.691 GPS Accuracy ± 13.1 ft.	Irrua specialist hospital was taken as the ending of Eguare region/location.
Emaudo Campus, AAU, X_1	Beginning of emaudo campus. A.A.U, Ekpoma	Mobile latitude 6^0 46'6.134" Mobile latitude $6^0$8'31.805" GPS Accuracy ± 26.2ft.	Some kilometers before the bus stop was taken as the beginning
Emaudo Campus, A.A.U X_2	Ending Nof emaudo campus	Mobile latitude 6^0 46'10.112" Mobile latitude $6^0$8'36.636 GPS Accuracy ± 26.1ft.	Soil science farm, was taken as the ending of ending of emaudo campus.
College of	Beginning of	Mobile latitude	Some kilometers before the

medicine campus, A.A.U C_1	college of medicine	$6^0 44'24.724''$ Mobile latitude $6^0 6'28.675$ GPS Accuracy ± 26.2ft	entrance gate was taken as the beginning of college of medicine

3.2. Equipment Used

RF signal tracker was used in this study in conjunction with a Samsung galaxy pocket phone of model: GT – 55300 (Fig.3.1). The mobile phone was used to detect the signal strength for the network while the RF signal tracker with software version 01, was used to determine the power reception level/signal strength level, in dBm and the location parameter and site parameters serving the studied location.

Device layout

Earpiece

Volume key

Touch screen

Home key

Back key

Option key

Microphone

Multifunction jack

Headset jack

Camera lens

GPS antenna[1]

Power/Reset/Lock key

Speaker

Back cover

Main antenna
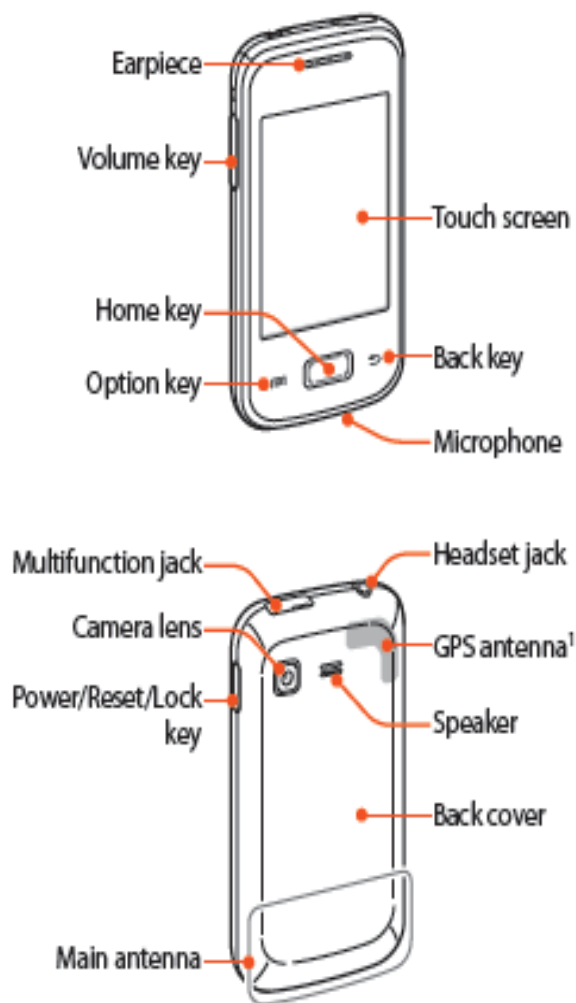
Fig.3.1: Samsung Galaxy Pocket

Table 3.3: RF Main Screen Menu

Phone Parameters.	
Number	08063268446
Phone type	GSM
IMEI/ESN	353170055933935
Manufacturer	Samsung
Model	GT-S5300
SIM SN	Nil
SIM State	STATE-READY
Software version	01
Sub ID	Nil
Signal strength	-75dBm
Bit Error Rate	255
EVDO	-1dBm
Ec/I_o	-1
SNR	-1
Battery level	80%
Network Parameters	
Operator	MTN
Technology	EDGE
MCC	621
MNC	Nil
LAC	30
Cell id	Nil

Location Parameters	
Site database	Nil
Best Provider	GPRS
Mobile latitude	Nil
Mobile longitude	Nil
Mobile Heading	Nil
Mobile Altitude	Nil
Site brg	Nil
Speed	Nil
GPS Accuracy	Nil
Distance to Site	Nil

During measurement, all phone parameters were constants except the signal strength and the battery level which varies from time to time while in network parameters, every other parameters were constant with only cell ID changing and in some cases remain constant before changing to another cell ID, in location parameters, in most cases, every other parameters remains constant with only the distance to site changing from time to time.

3.3. Measurement Procedure

The general approach was to measure the signal strength level of MTN network signal in the chosen locations (Ambrose Alli University, college of medicine, Emaudo Campus, A.A.U, Eguare Ekpoma and Ujoelen, Ekpoma, Edo State). The chosen locations attenuations were then computed.

The Samsung galaxy pocket handset and MTN SIM card were used to conduct the measurement.

Readings were taken only when there was a change in the distance to site indicated by the RF signal tracker. And these readings were taken from the beginning of any chosen location and the readings were recorded and the corresponding distances to sites and their signal strengths were also recorded.

The geographical location parameters and their descriptions were all recorded. These were taken from the beginning of the tested locations and the parameters included: mobile latitude, mobile longitude, mobile heading, site bearing, GPS accuracy and speed. The GPS function of the Samsung galaxy pocket must be switched ON before the RF signal tracker can work otherwise, it will fail to function.

3.4. Measurement Conditions

Measurements were taken five different times for each of the locations for a period of six months from 0ctober 2012 to March 2013. This was to allow a clear picture of the variation of the weather within the period of study.

3.5. Data Presentation

The signal strength and distance to site were measured and recorded in each of the tested locations. The distance was measured in miles and was later converted to kilometer with software called miles to kilometer converter. The Tables of the readings were as shown in Tables 3.4 to 3.27.

3.5.1. Power Received/Signal Strength And Distance To Site (Base Station) For Tested Location "College Of Medicine, Campus, A.A.U" Was As Shown From Table 3.4-3.9.

In this portion of the research, the signal strength over a given distance to site for college of medicine for the period of study was as shown in Tables 3.4 -3.9

Table 3.4: Measured Signal Strength For A Given Distance For The Month Of October 2012

DAYS	SIGNAL STRENGTH AT A GIVEN DISTANCE IN dBm.				
	1 km	2 km	3 km	4 km	5 km
1	-79	-81	-77	-81	-89
2	-89	-75	-89	-85	-81
3	-79	-75	-75	-73	-79
4	-91	-91	-89	-81	-63
5	-61	-89	-63	-65	-85
6	-91	-75	-77	-83	-81
7	-85	-75	-61	-83	-91
8	-65	-75	-71	-63	-73
9	-71	-75	-85	-91	-65
10	-63	-73	-75	-81	-85
11	-91	-93	-87	-83	-75
12	-75	-73	-61	-85	-93
13	-75	-75	-75	-73	-61
14	-91	-83	-81	-93	-77
15	-81	-81	-81	-83	-61
16	-63	-71	-75	-91	-69
17	-83	-81	-69	-91	-73
18	-77	-95	-85	-83	-89
19	-73	-77	-69	-85	-65
20	-79	-83	-69	-79	-91
21	-83	-79	-67	-73	-69
22	-77	-85	-83	-61	-91
23	-69	-73	-69	-91	-77
24	-79	-81	-81	-91	-67
25	-69	-89	-85	-93	-91
26	-77	-83	-81	-91	-73
27	-93	-89	-91	-69	-77
28	-91	-83	-79	-93	-82
29	-79	-79	-83	-69	-91
30	-73	-87	-91	-73	-89
31	-67	-67	-67	-93	-89
MEAN	-75.7	-77.9	81.4	-81.5	-78.8

Table 3.5: Measured Signal Strength For a Given Distance For The Month Of November 2012

DAYS	SIGNAL STRENGTH AT A GIVEN DISTANCE IN dBm.				
	1 km	2 km	3 km	4 km	5 km
1	-89	-69	-75	-81	79
2	-93	-79	-83	-69	-89
3	-85	-77	-69	-91	-75
4	-69	-81	-79	-83	-73
5	-91	-75	-77	-69	-81
6	-77	-79	-93	-93	-93
7	-69	-85	-89	-73	-91
8	-91	-93	-73	-85	-69
9	-67	-83	-91	-79	-69
10	-69	-67	-83	-85	-93
11	-91	-73	-71	-89	-91
12	-87	-87	-69	-91	-85
13	-77	-75	-89	-91	-91
14	-93	-91	-89	-87	-87
15	-87	-77	-69	-65	-71
16	-71	-85	-69	-77	-87
17	-85	-63	-79	-91	-93
18	-89	-69	-75	-95	-71
19	-67	-63	-69	-85	-71
20	-81	-79	-73	-93	-69
21	-77	-89	-83	-69	-91
22	-93	-93	-89	-87	-69
23	-71	-73	-91	-89	-77
24	-93	-91	-79	-85	-69
25	-77	-89	-81	-93	-61
26	-77	-85	-93	-69	-85
27	-77	-85	-69	-93	-89
28	-89	-79	-65	-91	-67
29	-85	-81	-71	-69	-77
30	-69	-69	-91	-89	-93
MEAN	-80.8	-79.7	-79.6	-83.8	-79.8

Table 3.6: Measured Signal Strength for a Given Distance For The Month Of December2012

DAYS	SIGNAL STRENGTH AT A GIVEN DISTANCE IN dBm.				
	1 km	2 km	3 km	4 km	5 km
1	-93	-81	-63	-51	-81
2	-77	-71	-89	-87	-73
3	-89	-91	-93	-77	-65
4	-68	-65	-69	-73	-71
5	-85	-89	-88	-69	-67
6	-61	-93	-95	-99	-65
7	-71	-73	-89	-69	-77
8	-73	-81	-67	-65	-61
9	-69	-73	-97	-77	-79
10	-83	-89	-87	-63	-69
11	-67	-78	-79	-63	-69
12	-93	-99	-81	-67	-63
13	-67	-68	-77	-93	-97
14	-95	-95	-95	-73	-69
15	-73	-77	-69	-67	-89
16	-75	-85	-65	-93	-79
17	-69	-63	-67	-65	-63
18	-69	-93	-97	-85	-89
19	-93	-73	-79	-68	-69
20	-77	-99	-63	-67	-69
21	-67	-69	-61	-89	-83
22	-89	-93	-97	-77	-73
23	-89	-93	-72	-73	-77
24	-69	-63	-65	-77	-75
25	-93	-97	-93	-89	-83
26	-65	-73	-69	-79	-89
27	-69	-81	-71	-87	-72
28	-73	-93	-77	-97	-69
29	-69	-79	-81	-87	-89
30	-87	-65	-77	-73	-69
31	-69	-81	-77	-73	-75
MEAN	-77.0	-81.4	-89.0	-76.5	-75.0

Table 3.7: Measured Signal Strength For a Given Distance For The Month Of January 2013

DAYS	SIGNAL STRENGTH AT A GIVEN DISTANCE IN dBm.				
	1 km	2 km	3 km	4 km	5 km
1	-77	-69	-83	-87	-89
2	-81	-89	-77	-73	-97
3	-95	-81	-89	-87	-69
4	-77	-89	-65	-67	-81
5	-97	-95	-93	-77	-75
6	-97	-93	-83	-89	-69
7	-77	-73	-71	-69	-63
8	-71	-78	-93	-97	-69
9	-89	-63	-79	-77	-73
10	-93	-73	-69	-89	-89
11	-89	-79	-73	-77	-67
12	-81	-83	-83	-83	-83
13	-91	-69	-65	-77	-73
14	-93	-91	-81	-65	-81
15	-73	-75	-69	-77	-69
16	-89	-83	-77	-73	-65
17	-97	-95	-93	-67	-69
18	-93	-97	-63	-73	-89
-81	-77	-65	-89	-67	-81
20	-93	-93	-93	-93	-89
21	-77	-69	-81	-83	-67
22	-89	-89	-91	-61	-97
23	-93	-61	-79	-69	-73
24	-61	-63	-81	-83	-83
25	-83	-71	-77	-93	-99
26	-87	-61	-65	-73	-99
27	-81	-93	-83	-81	-91
28	-93	-99	-87	-81	-89
29	-67	-61	-65	-63	-61
30	-55	-81	-93	-97	-93
31	-87	-73	-75	-77	-61
MEAN	-85.9	-79.2	-79.5	-78.2	-79.1

Table 3.8: Measured Signal Strength For a Given Distance For The Month Of February 2013

DAYS	SIGNAL STRENGTH AT A GIVEN DISTANCE IN dBm.				
	1 km	2 km	3 km	4 km	5 km
1	-73	-73	-91	-93	-95
2	-71	-81	-83	-75	-77
3	-73	-75	-79	-79	-75
4	-91	-91	-89	-87	-87
5	-77	-75	-81	-93	-95
6	-79	-89	-83	-85	-87
7	-79	-73	-71	-77	-75
8	-73	-95	-81	-91	-89
9	-71	-83	-73	-81	-73
10	-77	-85	-93	-81	-89
11	-93	-91	-95	-95	-89
12	-89	-89	-87	-85	-81
13	-79	-91	-89	-77	-81
14	-87	-73	-85	-79	-91
15	-89	-73	-83	-75	-79
16	-85	-73	-91	-71	-95
17	-71	-89	-73	-91	-81
18	-83	-89	-71	-91	-93
19	-85	-79	-81	-89	-73
20	-81	-75	-93	-91	-95
21	-75	-83	-81	-73	-83
22	-71	-95	-89	-91	-93
23	-91	-73	-81	-71	-87
24	-95	-77	-93	-75	-91
25	-71	-77	-81	-91	-93
26	-77	-95	-71	-73	-89
27	-71	-81	-89	-91	-93
28	-95	-91	-79	-71	-73
MEAN	-80.4	-82.6	83.4	-82.9	-85.8

Table 3.9: Measured Signal Strength For a Given Distance For The Month Of March 2013

DAYS	SIGNAL STRENGTH AT A GIVEN DISTANCE IN dBm.				
	1 km	2 km	3 km	4 km	5 km
1	-91	-73	-81	-71	-83
2	-81	-89	-91	-95	-93
3	-91	-89	-93	-77	-73
4	-75	-71	-81	-91	-93
5	-93	-89	-95	-83	-85
6	-71	-73	-81	-91	-89
7	-91	-89	-95	-71	-81
8	-89	-75	-91	-81	-77
9	-81	-71	-95	-91	-95
10	-97	-81	-71	-77	-75
11	-77	-73	-71	-85	-77
12	-91	-71	-73	-81	-75
13	-91	-93	-81	-79	-75
14	-91	-79	-81	-89	-85
15	-95	-93	-89	-77	-71
16	-91	-93	-93	-89	-89
17	-85	-91	-87	-77	-71
18	-75	-73	-81	-95	-95
19	-91	-77	-95	-89	-71
20	-73	-93	-95	-93	-85
21	-71	-73	-93	-95	-91
22	-89	-71	-77	-81	-89
23	-81	-73	-83	-91	-95
24	-93	-71	-73	-91	-93
25	-93	-95	-91	-81	-71
26	-77	-81	-89	-81	-91
27	-91	-93	-89	-71	-77
28	-73	-71	-81	-91	-93
29	-93	-87	-67	-55	-89
30	-65	-87	-61	-79	-99
31	-67	-67	-91	-87	-87
MEAN	-84.3	-80.8	-84.4	-83.4	-86.6

3.5.2. Power received/signal strength and distance to site (base station) for tested location ''Ujoelen, Ekpoma'' is shown from Tables 3.10-3.15

Table 3.10: Measured Signal Strength For a Given Distance For The Month Of October 2012

DAYS	SIGNAL STRENGTH AT A GIVEN DISTANCE IN dBm.				
	1 km	2 km	3 km	4 km	5 km
1	-73	-61	-61	-67	-71
2	-63	-63	-67	-59	-63
3	-67	-93	-91	-89	-87
4	-93	-95	-95	-93	-95
5	-89	-67	-91	-93	-93
6	-87	-95	-95	-93	-95
7	-71	-67	-61	-61	-73
8	-67	-63	-63	-63	-69
9	-57	-85	-81	-77	-80
10	-89	-95	-90	-88	-90
11	-98	-99	-80	-92	-81
12	-87	-91	-80	-67	-91
13	-88	-89	-75	-88	-71
14	-66	-92	-77	-80	-83
15	-67	-84	-79	-82	-84
16	-91	-87	-81	-84	-61
17	-53	-85	-95	-89	-82
18	-91	-93	-84	-91	-93
19	-51	-75	-61	-74	-70
20	-52	-65	-80	-71	-89
21	-59	-51	-53	-57	-62
22	-69	-80	-89	-72	-59
23	-60	-69	-72	-54	-73
24	-90	-84	-55	-55	-67
25	-80	-83	-59	-60	-52
26	-90	-94	-95	-51	-58
27	-81	-90	-52	-77	-61
28	-84	-57	-99	-95	-93
29	-57	-59	-66	-72	-92
30	-55	-51	-66	-80	-91
31	-63	-67	-92	-51	-81
MEAN	-73.8	-73.4	-76.9	-75.0	-77.7

Table 3.11: Measured Signal Strength For a Given Distance For The Month Of November 2012

DAYS	SIGNAL STRENGTH AT A GIVEN DISTANCE IN dBm.				
	1 km	2 km	3 km	4 km	5 km
1	-81	-50	-62	-82	-94
2	-67	-77	-51	-80	-91
3	-93	-93	-79	-63	-94
4	-57	-67	-63	-63	-63
5	-63	-71	-73	-90	-80
6	-63	-57	-53	-80	-83
7	-77	-71	-73	-79	-65
8	-90	-90	-90	-91	-82
9	-77	-52	-68	-81	-92
10	-63	-67	-53	-50	-51
11	-87	-82	-77	-72	-72
12	-90	-94	-89	-72	-52
13	-61	-51	-60	-82	-59
14	-61	-61	-61	-67	-73
15	-63	-63	-67	-53	-64
16	-75	-61	-61	-65	-70
17	-63	-63	-67	-58	-63
18	-70	-61	-61	-65	-81
19	-71	-63	-62	-59	-62
20	-92	-57	-69	-72	-67
21	-62	-85	-52	-67	-61
22	-70	-98	-92	-81	-53
23	-71	-67	-61	-51	-53
24	-53	-61	-61	-72	-72
25	-72	-51	-94	-83	-63
26	-72	-72	-51	-53	-57
27	-83	-77	-80	-99	-93
28	-53	-57	-61	-72	-77
29	-64	-70	-66	-88	-92
30	-81	-83	-53	-67	-59
MEAN	-71.2	-69.0	-67.0	-71.7	-71.0

Table 3.12: Measured Signal Strength For a Given Distance For The Month Of December 2012

DAYS	SIGNAL STRENGTH AT A GIVEN DISTANCE IN dBm.				
	1 km	2 km	3 km	4 km	5 km
1	-51	-57	-73	-75	-77
2	-93	-97	-61	-63	-63
3	-57	-57	-69	-67	-57
4	-87	-81	-89	-91	-93
5	-63	-63	-67	-67	-67
6	-69	-81	-83	-53	-57
7	-83	-83	-87	-59	-57
8	-61	-73	-75	-93	-99
9	-71	-81	-53	-57	-93
10	-69	-81	-61	-89	-71
11	-81	-93	-51	-59	-67
12	-53	-93	-81	-97	-99
13	-97	-93	-95	-91	-91
14	-91	-53	-51	-55	-61
15	-63	-67	-67	-53	-53
16	-59	-71	-77	-91	-93
17	-71	-77	-59	-57	-53
18	-83	-85	-91	-99	-93
19	-91	-93	-93	-93	-59
20	-61	-61	-83	-89	-87
21	-81	-73	-61	-77	-59
22	-61	-67	-91	-59	-95
23	-73	-95	-81	-91	-53
24	-97	-61	-93	-73	-99
25	-93	-91	-91	-91	-51
26	-81	-83	-83	-85	-87
27	-51	-51	-89	-61	-77
28	-81	-83	-59	-69	-91
29	-63	-63	-67	-59	-73
30	-73	-77	-79	-91	-93
31	-91	-61	-89	-59	-51
MEAN	-74.2	-75.6	-75.8	-76.5	-74.8

Table 3.13: Measured Signal Strength For a Given Distance For The Month Of January 2013

DAYS	SIGNAL STRENGTH AT A GIVEN DISTANCE IN dBm.				
	1 km	2 km	3 km	4 km	5 km
1	-79	-81	-83	-71	-73
2	-81	-59	-71	-61	-93
3	-73	-81	-83	-59	-61
4	-93	-81	-89	-53	-89
5	-81	-69	-67	-63	-61
6	-57	-53	-61	-73	-91
7	-61	-81	-63	-71	-65
8	-61	-71	-73	-63	-89
9	-83	-65	-81	-73	-91
10	-71	-73	-73	-73	-73
11	-81	-83	-85	-61	-63
12	-93	-53	-71	-61	-81
13	-93	-99	-59	-67	-69
14	-61	-59	-61	-73	-91
15	-93	-89	-99	-89	-81
16	-63	-71	-91	-81	-89
17	-73	-73	-61	-59	-79
18	-61	-65	-63	-75	-57
19	-73	-93	-71	-81	-91
20	-99	-81	-51	-57	-53
21	-91	-61	-73	-81	-57
22	-61	-63	-65	-71	-73
23	-77	-81	-91	-93	-99
24	-93	-71	-91	-51	-81
25	-59	-61	-73	-87	-81
26	-91	-51	-93	-89	-71
27	-93	-65	-53	-61	-81
28	-53	-57	-91	-71	-81
29	-83	-91	-63	-61	-99
30	-53	-63	-67	-61	-81
31	-59	-93	-75	-79	-89
MEAN	-75.6	-72.2	-73.9	-69.6	-78.5

Table 3.14: Measured Signal Strength For a Given Distance For The Month Of February 2013

DAYS	SIGNAL STRENGTH AT A GIVEN DISTANCE IN dBm.				
	1 km	2 km	3 km	4 km	5 km
1	-95	-61	-67	-93	-97
2	-59	-81	-51	-73	-69
3	-71	-93	-61	-89	-85
4	-69	-93	-63	-89	-69
5	-81	-71	-83	-79	-81
6	-97	-91	-93	-55	-81
7	-55	-53	-61	-63	-71
8	-89	-93	-95	-75	-55
9	-61	-71	-85	-89	-93
10	-91	-93	-85	-83	-89
11	-61	-81	-91	-93	-89
12	-61	-97	-63	-65	-67
13	-69	-93	-71	-67	-79
14	-63	-61	-91	-69	-81
15	-63	-79	-55	-77	-73
16	-55	-61	-93	-91	-65
17	-63	-81	-97	-65	-89
18	-93	-69	-79	-63	-73
19	-69	-89	-63	-73	-65
20	-67	-93	-81	-83	-97
21	-65	-53	-71	-59	-77
22	-55	-65	-59	-81	-89
23	-81	-51	-53	-73	-55
24	-57	-75	-63	-69	-93
25	-63	-73	-55	-52	-61
26	-87	-63	-61	-95	-67
27	-89	-55	-57	-63	-67
28	-97	-87	-67	-53	-61
MEAN	-72.4	-75.9	-71.9	-74.3	-76.4

Table 3.15: Measured Signal Strength For a Given Distance For The Month Of March 2013

DAYS	SIGNAL STRENGTH AT A GIVEN DISTANCE IN dBm.				
	1 km	2 km	3 km	4 km	5 km
1	-51	-53	-73	-77	-71
2	-63	-65	-61	-89	-83
3	-89	-51	-93	-57	-91
4	-59	-63	-61	-67	-69
5	-57	-61	-89	-83	-93
6	-91	-67	-69	-51	-61
7	-93	-69	-67	-63	-59
8	-57	-53	-69	-83	-83
9	-69	-83	-81	-79	-77
10	-93	-53	-59	-67	-69
11	-83	-91	-93	-91	-63
12	-65	-63	-59	-51	-53
13	-61	-61	-59	-51	-53
14	-83	-79	-77	-91	-89
15	-91	-61	-89	-69	-63
16	-61	-69	-77	-63	-71
17	-93	-95	-93	-91	-83
18	-87	-81	-61	-53	-55
19	-79	-63	-61	-85	-83
20	-73	-81	-75	-61	-95
21	-83	-73	-79	-91	-67
22	-71	-93	-63	-81	-89
23	-61	-77	-63	-83	-69
24	-71	-91	-61	-93	-97
25	-63	-71	-79	-69	-75
26	-77	-67	-89	-81	-93
27	-59	-71	-65	-55	-93
28	-89	-63	-81	-97	-69
29	-51	-59	-63	-57	-67
30	-69	-63	-77	-63	-73
31	-83	-63	-85	-81	-69
MEAN	-73.3	-69.5	-73.1	-73.3	-75.0

3.5.3. Power received/signal strength and distance to site (base station) for tested location ''Egaure, Ekpoma'' is shown from Tables 3.16-3.21

Table 3.16: Measured Signal Strength For a Given Distance For The Month Of October, 2012.

DAYS	SIGNAL STRENGTH AT A GIVEN DISTANCE IN dBm.				
	1 km	2 km	3 km	4 km	5 km
1	-67	-69	-69	-61	-51
2	-53	-55	-51	-59	-57
3	-67	-63	-65	-59	-51
4	-55	-51	-55	-51	-53
5	-66	-65	-67	-58	-51
6	-57	-63	-61	-63	-53
7	-53	-57	-55	-63	-65
8	-59	-68	-53	-54	-61
9	-65	-67	-67	-51	-53
10	-61	-53	-51	-58	-57
11	-66	-53	-51	-61	-63
12	-69	-61	-67	-63	-51
13	-62	-54	-61	-67	-59
14	-62	-65	-63	-50	-57
15	-55	-62	-61	-53	-51
16	-62	-62	-62	-62	-59
17	-57	-65	-67	-53	-53
18	-55	-52	-65	-67	-51
19	-61	-57	-57	-53	-53
20	-61	-65	-53	-51	-62
21	-51	-57	-65	-55	-57
22	-59	-60	-60	-63	-67
23	-51	-53	-63	-67	-66
24	-52	-51	-64	-66	-65
25	-63	-53	-50	-52	-61
26	-57	-63	-61	-51	-50
27	-61	-55	-54	-63	-67
28	-58	-55	-51	-63	-61
29	-53	-52	-62	-61	-67
30	-55	-57	-61	-53	-51
31	-67	-63	-68	-52	-53
MEAN	-61.0	-56.9	-60.0	-60.2	-55.4

Table 3.17: Measured Signal Strength For a Given Distance For The Month Of November, 2012

DAYS	SIGNAL STRENGTH AT A GIVEN DISTANCE IN dBm.				
	1 km	2 km	3 km	4 km	5 km
1	-62	-63	-51	-51	-51
2	-57	-59	-60	-61	-67
3	-52	-57	-57	-57	-60
4	-61	-67	-52	-60	-53
5	-61	-53	-51	-57	-64
6	-63	-67	-54	-60	-59
7	-53	-53	-55	-63	-67
8	-57	-63	-60	-59	-53
9	-65	-67	-61	-52	-60
10	-51	-53	-57	-60	-61
11	-64	-63	-61	-60	-55
12	-54	-53	-57	-69	-62
13	-52	-51	-51	-60	-50
14	-51	-61	-63	-50	-57
15	-60	-51	-67	-69	-51
16	-53	-55	-67	-63	-60
17	-63	-61	-52	-50	-60
18	-60	-63	-50	-62	-67
19	-50	-52	-61	-63	-51
20	-60	-69	-69	-79	-67
21	-53	-51	-67	-60	-57
22	-60	-55	-50	-63	-53
23	-55	-65	-60	-67	-53
24	-57	-50	-63	-66	-64
25	-63	-60	-50	-57	-53
26	-63	-52	-53	-63	-77
27	-61	-55	-50	-57	-51
28	-67	-55	-62	-63	-61
29	-77	-52	-67	-59	-67
30	-55	-57	-71	-53	-57
MEAN	-59.0	-57.7	-57.8	-60.2	-58.4

Table 3.18: Measured Signal Strength For a Given Distance For The Month Of December 2012

DAYS	SIGNAL STRENGTH AT A GIVEN DISTANCE IN dBm.				
	1 km	2 km	3 km	4 km	5 km
1	-61	-63	-63	-63	-63
2	-63	-57	-57	-59	-61
3	-63	-65	-61	-67	-67
4	-67	-51	-63	-63	-63
5	-63	-63	-63	-67	-67
6	-67	-51	-53	-53	-57
7	-63	-51	-57	-63	-65
8	-59	-57	-55	-67	-69
9	-65	-61	-65	-63	-67
10	-63	-53	-51	-55	-63
11	-51	-63	-65	-53	-57
12	-59	-57	-51	-61	-63
13	-51	-53	-51	-57	-69
14	-65	-53	-53	-69	-61
15	-69	-69	-69	-65	-53
16	-57	-51	-53	-53	-61
17	-55	-53	-51	-51	-53
18	-65	-53	-51	-57	-57
19	-51	-69	-67	-61	-63
20	-61	-61	-51	-57	-53
21	-59	-65	-67	-55	-65
22	-67	-67	-65	-55	-63
23	-53	-61	-67	-55	-57
24	-63	-61	-65	-61	-67
25	-53	-63	-61	-67	-69
26	-61	-63	-59	-57	-58
27	-51	-63	-63	-63	-69
28	-57	-57	-57	-51	-61
29	-63	-55	-51	-53	-61
30	-63	-63	-63	-65	-67
31	-69	-69	-59	-53	-57
MEAN	-60.5	-59.4	-58.9	-59.3	-62.1

Table 3.19: Measured Signal Strength For a Given Distance For The Month Of January, 2013

DAYS	SIGNAL STRENGTH AT A GIVEN DISTANCE IN dBm.				
	1 km	2 km	3 km	4 km	5 km
1	-51	-55	-55	-59	-69
2	-61	-61	-63	-63	-69
3	-63	-51	-57	-59	-63
4	-61	-61	-67	-53	-57
5	-53	-53	-57	-69	-53
6	-69	-53	-69	-67	-65
7	-61	-63	-65	-65	-65
8	-65	-61	-67	-59	-59
9	-61	-63	-63	-65	-65
10	-69	-59	-55	-57	-63
11	-57	-57	-57	-61	-63
12	-65	-63	-61	-59	-57
13	-57	-51	-53	-57	-53
14	-61	-69	-51	-53	-69
15	-53	-53	-53	-59	-61
16	-61	-63	-69	-59	-57
17	-61	-63	-51	-57	-59
18	-53	-53	-57	-59	-61
19	-63	-65	-67	-67	-67
20	-59	-59	-57	-61	-63
21	-53	-55	-55	-61	-65
22	-63	-63	-69	-69	-69
23	-53	-51	-59	-59	-61
24	-69	-63	-61	-61	-61
25	-61	-63	-61	-61	-67
26	-63	-61	-65	-61	-63
27	-59	-61	-63	-69	-67
28	-69	-51	-67	-53	-69
29	-53	-53	-67	-63	-59
30	-67	-59	-63	-67	-63
31	-59	-57	-51	-65	-67
MEAN	-60.4	-58.5	-60.5	-61.2	-62.9

Table 3.20: Measured Signal Strength For a Given Distance For The Month Of February 2013

DAYS	SIGNAL STRENGTH AT A GIVEN DISTANCE IN dBm.				
	1 km	2 km	3 km	4 km	5 km
1	-67	-59	-59	-61	-63
2	-65	-51	-51	-59	-57
3	-53	-57	-69	-67	-63
4	-53	-59	-51	-61	-67
5	-61	-57	-63	-63	-65
6	-67	-59	-57	-51	-61
7	-59	-53	-61	-59	-51
8	-69	-57	-63	-69	-61
9	-53	-57	-59	-61	-59
10	-53	-63	-67	-61	-69
11	-61	-63	-67	-59	-53
12	-57	-61	-57	-51	-53
13	-69	-61	-59	-53	-61
14	-57	-63	-51	-59	-67
15	-69	-67	-59	-63	-61
16	-63	-53	-67	-69	-59
17	-61	-53	-63	-59	-69
18	-57	-67	-63	-65	-59
19	-63	-61	-63	-59	-69
20	-53	-59	-53	-57	-69
21	-67	-63	-63	-57	-53
22	-69	-53	-63	-57	-69
23	-61	-59	-63	-51	-51
24	-63	-53	-69	-67	-61
25	-63	-53	-57	-51	-69
26	-51	-53	-63	-57	-67
27	-61	-63	-63	-59	-61
28	-59	-69	-67	-59	-63
MEAN	-56.8	-58.8	-62.9	-59.4	-61.8

Table 3.21: Measured Signal Strength For a Given Distance For The Month Of March 2013

DAYS	SIGNAL STRENGTH AT A GIVEN DISTANCE IN dBm.				
	1 km	2 km	3 km	4 km	5 km
1	-57	-63	-69	-53	-57
2	-59	-69	-63	-53	-59
3	-61	-63	-61	-69	-69
4	-63	-61	-63	-69	-61
5	-51	-59	-61	-51	-63
6	-59	-59	-63	-57	-67
7	-67	-61	-57	-53	-55
8	-67	-69	-63	-67	-59
9	-53	-63	-61	-61	-63
10	-69	-59	-67	-57	-69
11	-69	-59	-61	-57	-63
12	-67	-63	-57	-53	-69
13	-57	-59	-69	-53	-51
14	-65	-67	-63	-59	-61
15	-67	-65	-69	-63	-65
16	-61	-59	-59	-67	-61
17	-51	-67	-53	-57	-53
18	-69	-57	-61	-51	-59
19	-51	-53	-57	-67	-63
20	-59	-69	-67	-69	-61
21	-67	-53	-61	-61	-69
22	-63	-53	-61	-59	-61
23	-51	-57	-59	-63	-67
24	-69	-59	-61	-53	-67
25	-69	-53	-57	-61	-63
26	-69	-59	-51	-69	-67
27	-61	-55	-50	-57	-51
28	-67	-65	-62	-55	-69
29	-67	-55	-67	-59	-67
30	-67	-63	-59	-61	-57
31	-57	-63	-69	-59	-51
MEAN	-64.5	-60.6	-61.3	-59.5	-61.8

3.5.4. Power received/signal strength and distance to site (base station) for tested location ''Emaudo Ekpoma'' is shown from Tables 3.22 – 3.27.

Table 3.22: Measured Signal Strength For a Given Distance For The Month Of October, 2012.

DAYS	SIGNAL STRENGTH AT A GIVEN DISTANCE IN dBm.				
	1 km	2 km	3 km	4 km	5 km
1	-75	-73	-87	-87	-95
2	-95	-93	-89	-91	-91
3	-67	-63	-85	-85	-83
4	-81	-85	-83	-65	-71
5	-75	-73	-83	-93	-69
6	-73	-81	-85	-93	-95
7	-95	-73	-63	-65	-85
8	-93	-93	-85	-73	-85
9	-95	-95	-67	-61	-93
10	-61	-67	-65	-93	-75
11	-81	-83	-97	-67	-73
12	-65	-69	-73	-63	-95
13	-93	-81	-69	-63	-77
14	-62	-65	-93	-91	-75
15	-91	-89	-63	-67	-97
16	-91	-63	-69	-73	-75
17	-63	-85	-90	-72	-60
18	-73	-79	-93	-85	-62
19	-73	-61	-73	-95	-77
20	-77	-73	-95	-97	-67
21	-81	-89	-69	-95	-91
22	-71	-79	-63	-67	-61
23	-71	-95	-81	-87	-91
24	-65	-63	-81	-75	-91
25	-73	-77	-75	-97	-79
26	-93	-95	-85	-89	-81
27	-61	-63	-77	-93	-85
28	-69	-67	-85	-87	-83
29	-71	-73	-61	-73	-87
30	-93	-91	-61	-63	95
31	-69	-71	-93	-95	-65
MEAN	-77.3	-77.6	-78.6	-80.0	-80.9

Table 3.23: Measured Signal Strength For a Given Distance For The Month Of November, 2012

DAYS	SIGNAL STRENGTH AT A GIVEN DISTANCE IN dBm.				
	1 km	2 km	3 km	4 km	5 km
1	-87	-87	-91	-89	-81
2	-75	-93	-85	-69	-73
3	-95	-97	-71	-75	-61
4	-73	-93	-95	-81	-73
5	-65	-71	-95	-81	-83
6	-97	-63	-61	-69	-71
7	-73	-93	-65	-85	-73
8	-81	-75	-63	-71	-75
9	-85	-81	-77	-67	-95
10	-73	-63	-61	-83	-91
11	-93	-65	-83	-91	-61
12	-93	-85	-87	-73	-77
13	-73	-73	-97	-60	-65
14	-63	-81	-87	-73	-95
15	-71	-71	-69	-83	-61
16	-74	-66	-93	-99	-60
17	-81	-70	-95	-62	-98
18	-67	-69	-90	-76	-77
19	-69	-65	-93	-65	-77
20	-85	-83	-93	-75	-87
21	-77	-69	-77	-65	-63
22	-85	-89	-91	-93	-95
23	-99	-69	-76	-63	-75
24	-81	-67	-63	-75	-87
25	-71	-73	-63	-95	-91
26	-77	-63	-67	-63	-61
27	-89	-87	-81	-65	-67
28	-91	-93	-99	-77	-71
29	-77	-93	-91	-63	-67
30	-71	-77	-87	-89	-99
MEAN	-79.2	-77.8	-81.6	-75.7	-76.9

Table 3.24: Measured Signal Strength For a Given Distance For The Month Of December, 2012

DAYS	SIGNAL STRENGTH AT A GIVEN DISTANCE IN dBm.				
	1 km	2 km	3 km	4 km	5 km
1	-71	-75	-79	-71	-91
2	-93	-91	-99	-95	-93
3	-71	-73	71	-69	-77
4	-87	-87	-87	-69	-69
5	-93	-81	-73	-69	-83
6	-61	-61	-83	-83	-89
7	-71	-81	-82	-89	91
8	-87	-78	-93	-97	-73
9	-81	-89	-71	-73	-79
10	-71	-68	-78	-89	-97
11	-75	-77	-89	-81	-93
12	-93	-93	-83	-67	-79
13	-93	-93	-85	-81	-61
14	-75	-95	-89	-81	-71
15	-71	-83	-83	-83	-97
16	-91	-61	-89	-61	-81
17	-93	-95	-95	-95	-73
18	-93	-83	-89	-89	-91
19	-81	-97	-97	-95	-83
20	-81	-81	-93	-69	-95
21	-77	-73	-71	-89	-81
22	-81	-81	-73	-69	-71
23	-91	-97	-87	-63	-77
24	-63	-63	-65	-67	-89
25	-73	-75	-75	-93	-99
26	-85	-89	-73	-97	-93
27	-71	-69	-91	-93	-89
28	-83	-83	-83	-87	-91
29	-78	-83	-73	-91	-97
30	-93	-93	-87	-77	93
31	-69	-71	-93	-95	-91
MEAN	-80.5	-81.3	-83.2	-81.5	-85.1

Table 3.25: Measured Signal Strength For a Given Distance For The Month Of January 2013

DAYS	SIGNAL STRENGTH AT A GIVEN DISTANCE IN dBm.				
	1 km	2 km	3 km	4 km	5 km
1	-89	-87	-81	-83	-73
2	-81	-87	-83	-71	-89
3	-89	-93	-99	-91	-81
4	-69	-69	-67	-77	-75
5	-83	-83	-91	-93	-99
6	-93	-97	-97	-95	-93
7	-93	-73	-89	-81	-69
8	-81	-83	-89	-89	-79
9	-77	-79	-93	-97	-89
10	-93	-93	-89	-75	-69
11	-93	-99	-61	-63	-77
12	-65	-67	-81	-71	-77
13	-95	-95	-73	-77	-73
14	-73	-97	-89	-81	-83
15	-93	-89	-81	-83	-89
16	-73	-63	-73	-71	-69
17	-63	-73	-75	-69	-87
18	-71	-93	-61	-63	-69
19	-71	-81	-93	-95	-89
20	-73	-77	-89	-71	-69
21	-93	-71	-79	-81	-99
22	-81	-83	-91	-91	-93
23	-85	-73	-81	-91	-93
24	-71	-79	-91	-93	-95
25	-93	-95	-99	-89	-79
26	-97	-93	-69	-77	-71
27	-87	-81	-69	-73	-77
28	-69	-67	-77	-71	-73
29	-71	-75	-73	-87	-93
30	-67	-81	-83	-69	-97
31	-73	-93	-91	-89	-91
MEAN	-80.8	-82.9	-82.5	-80.9	-82.5

Table 3.26: Measured Signal Strength For a Given Distance For The Month Of February 2013

DAYS	SIGNAL STRENGTH AT A GIVEN DISTANCE IN dBm.				
	1 km	2 km	3 km	4 km	5 km
1	-74	-83	-81	-93	-71
2	-84	-82	-73	-79	-96
3	-87	-96	-85	-91	-78
4	-82	-75	-81	-72	-89
5	-75	-93	-77	-83	-99
6	-74	-92	-89	-75	-95
7	-73	-91	-84	-87	-92
8	-71	-84	-71	-91	-83
9	-71	-77	-67	-95	-82
10	-87	-74	-83	-77	-89
11	-73	-75	-81	-89	-91
12	-79	-98	-77	-84	-83
13	-71	-71	-97	-93	-95
14	-81	-74	-88	-84	-75
15	-91	-94	-83	-76	-87
16	-71	-81	-84	-95	-73
17	-74	-72	-96	-84	-76
18	-83	-74	-89	-79	-91
19	-99	-84	-78	-97	-73
20	-82	-71	-84	-77	-83
21	-71	-84	-74	-79	-79
22	-76	-94	-74	-91	-83
23	-79	-73	-84	-80	-97
24	-74	-77	-82	-71	-89
25	-73	-94	-82	-79	-83
26	-94	-83	-96	-81	-88
27	-92	-90	-83	-94	-78
28	-74	-83	-97	-73	-91
MEAN	-79.1	-82.8	-82.9	-83.9	-85.3

Table 3.27: Measured Signal Strength For a Given Distance For The Month Of March 2013

DAYS	SIGNAL STRENGTH AT A GIVEN DISTANCE IN dBm.				
	1 km	2 km	3 km	4 km	5 km
1	-78	-91	-86	-89	-99
2	-81	-90	-72	-74	-83
3	-85	-94	-73	-81	-74
4	-82	-75	-81	-72	-79
5	-75	-93	-77	-83	-78
6	-97	-87	-84	-85	-88
7	-95	-75	-79	-75	-78
8	-89	-85	-76	-92	-85
9	-87	-84	-75	-96	-99
10	-81	-93	-87	-92	-98
11	-91	-79	-73	-71	-72
12	-85	-87	-97	-74	-78
13	-98	-87	-81	-92	-74
14	-77	-85	-81	-91	-94
15	-85	-77	-79	-95	-74
16	-87	-75	-78	-91	-93
17	-85	-91	-89	-78	-83
18	-84	-73	-94	-99	-82
19	-93	-79	-81	-89	-82
20	-94	-92	-98	-77	-75
21	-94	-92	-71	-86	-89
22	-76	-81	-97	-80	-84
23	-82	-75	-99	-77	-91
24	-90	-92	-98	-99	-81
25	-73	-87	-96	-99	-84
26	-91	-72	-97	-74	-70
27	-87	-74	-79	-75	-81
28	-84	-84	-97	-91	-75
29	-87	-89	-67	-78	-99
30	-97	-73	-89	-65	-89
31	-77	-67	-97	-87	-91
MEAN	-85.4	-83.2	-84.8	-84.1	-83.9

3.6. Mean of The Signal Strength/Received Power For The Different Months.

This portion of the research work shows the mean of the signal strength/received power at different distances. The mean of signal strength was calculated by adding the values of the signal strength received on each day of the month and divided by the number of days in the particular month. The mean of the different months were as shown in Tables 3.28 – 3.33.

3.6.1. Mean of the measured received signal strength for a given distance for the month of October, 2012.

Table 3.28: This shows the mean at each distance of the four different tested locations, College of medicine, AAU, Emaudo campus, AAU, Ujoelen Ekpoma and Eguare Ekpoma.

Distance (km)	1 km	2 km	3 km	4 km	5 km	Overall
College of medicine,AAU	-75.7	-77.9	-81.4	-81.5	-78.8	-78.54
Ujoelen	-73.8	-73.4	-76.9	-75.0	-77.7	-75.36
Eguare	-61.0	-56.9	-60.1	-60.2	-55.4	-58.72
Emaudo	-77.3	-77.6	-78.6	-80.0	-80.9	-78.88

3.6.2. Mean of the measured received signal strength for a given distance for the month of November, 2012.

Table 3.29: This shows the mean at each distance of the four different tested locations, College of medicine, AAU, Emaudo campus, AAU, Ujoelen Ekpoma and Eguare Ekpoma.

Distance (km)	1 km	2 km	3 km	4 km	5 km	Overall
College of Medicine, AAU	-80.8	-79.7	-79.6	-83.8	-79.8	-80.74
Ujoelen	-71.2	-69.0	-67.0	-71.7	-71.0	-69.98
Eguare	-59.0	-57.7	-57.8	-60.2	-58.4	-58.62
Emaudo	-79.2	-77.8	-81.6	-75.7	-76.9	-78.24

3.6.3. Mean of the measured received signal strength for a given distance for the month of December, 2012.

Table 3.30: This shows the mean at each distance of the four different tested locations, College of medicine, AAU, Emaudo campus, AAU, Ujoelen Ekpoma and Eguare Ekpoma.

Distance (km)	1 km	2 km	3 km	4 km	5 km	Overall
College of medicine ,AAU	-77.0	-81.4	-89.0	-76.5	-75.0	-79.78
Ujoelen	-74.2	-75.6	-75.8	-76.5	-74.8	-75.38
Eguare	-60.5	-59.4	-58.9	-59.3	-62.1	-60.04
Emaudo	-80.5	-81.3	-83.2	-81.5	-85.1	-82.32

3.6.4. Mean of the measured received signal strength for a given distance for the month of January, 2013.

Table 3.31: This shows the mean at each distance of the four different tested locations, College of medicine, AAU, Emaudo campus, AAU, Ujoelen Ekpoma and Eguare Ekpoma.

Distance (km)	1km	2km	3km	4km	5km	Overall
College of medicine, AAU	-85.9	-79.2	-79.5	-78.2	79.1	-80.38
Ujoelen	-75.6	-72.2	-73.9	-69.6	-78.5	-73.96
Eguare	-60.4	-58.5	-60.5	-61.2	-62.9	-60.70
Emaudo	-80.8	-82.5	-82.5	-80.9	-82.5	-81.84

3.6.5. Mean of the measured received signal strength for a given distance for the month of February, 2013.

Table 3.32: This shows the mean at each distance of the four different tested locations, College of medicine, AAU, Emaudo campus, AAU, Ujoelen Ekpoma and Eguare Ekpoma.

Distance (km)	1 km	2 km	3 km	4 km	5 km	Overall
College of Medicine, AAU	-80.4	-82.6	-83.4	-82.9	-85.8	83.0
Ujoelen	-72.4	-75.9	-71.9	-74.3	-76.4	74.2
Eguare	-56.8	-58.8	-62.9	-59.4	-61.8	59.9
Emaudo	-79.1	-82.8	-82.9	-83.9	-85.3	82.8

3.6.6. Mean of the measured received signal strength for a given distance for the month of March, 2013.

Table 3.33: This shows the mean at each distance of the four different tested locations, College of medicine, AAU, Emaudo campus, AAU, Ujoelen Ekpoma and Eguare Ekpoma.

Distance (km)	1 km	2 km	3 km	4 km	5 km	Overall
College of medicine	-84.3	-80.8	-84.4	-83.4	-86.6	83.9
Ujoelen	-73.3	-69.5	-73.1	-73.3	-75.0	72.8
Eguare	-64.5	-60.6	-61.3	-59.5	-61.8	61.5
Emaudo	-85.4	-83.2	-84.8	-84.1	-83.9	84.3

3.7. Calculation of Signal

This portion of this research deals with determination of signal and it is based on classical theories and empirical data which were collected from measurements, the classical theory is on the log-distance path loss model. The mean value of the path loss exponent for a shadow urban cellular radio was taken for the outdoor calculation/computation. Empirical data gotten were used to derive the model.

These data included;

(i) The received signal strength denoted by P_r

(ii) The transmitter-receiver separation distance which is taken as 100m denoted by d_0

3.8. Outdoor Calculations.

By using log-distance path loss model, the path loss is given as (Thiago, 2001).

$$PL(dB) = 10\log\frac{p_t}{p_r} = 10\log\left[\frac{\lambda^2}{(4\pi)^2 d^2}\right]$$ 3.1

Operating frequency was taken as 1800MHz

Wavelength, λ = speed of light/frequency 3.2

$$\lambda = \frac{c}{f} = \frac{3\times10^8}{1800\times10^6} = 0.167m$$ and d_0 = 100m(which is the fixed distance)

$$PL(dB) = -10\log\left[\frac{0.167^2}{(4\times3.142)^2\times100^2}\right]$$

= 77.5 dB

$$PL(d_0) = \frac{77.5}{1000} = 0.0775\,dBm.$$

Note that,

Path loss, PL (dBm) = PL (d_0) + 10nlog$\left(\dfrac{d}{d_0}\right)$ 3.3

This equation is based on theoretical calculation for outdoor (Longley, 1978).

Note that, value of n = $\sum \dfrac{n}{2}$ 3.4

And n = the path loss exponent values for shadowed urban environment.

n = $\dfrac{3+5}{2} = 4$ (average value of n)

3.9. Calculation Of Path Loss Using Existing Equation (log-distance path loss model)

At distance d = 1km,

$$PL(dBm) = 0.0775 + 10 \times 4 \log\left(\frac{1000}{100}\right)$$

= 40.1dBm.

At distance d = 2km,

$$PL(dBm) = 0.0775 + 10(4) \log\left(\frac{2000}{100}\right)$$

= 52.1dBm.

At distance d = 3km,

$$PL(dBm) = 0.0775 + 10(4)\log\left(\frac{3000}{100}\right)$$

$$= 59.2\text{dBm}.$$

At distance d = 4km,

$$PL(dBm) = 0.0775 + 10(4)\log\left(\frac{4000}{100}\right)$$

$$= 64.2\text{dBm}.$$

At distance d = 5km,

$$PL(dBm) = 0.0775 + 10(4)\log\left(\frac{5000}{100}\right)$$

$$= 68.0\text{dBm}.$$

3.10. Generation of Mathematical Model.

This generated model was named Anyasi's model, which is written mathematically as;

$$PL(dBm) = PL(d_0) + U10n\log\left(\frac{d_i}{d_0}\right) \qquad 3.5$$

Where U = $Y_{(i-1)}$ for i = distance to site, 1km,2km,3km,4km,5km…..nkm.

Y = modeled loss constant $= \dfrac{measure \quad received\,power}{calculated \quad power}$ \qquad 3.6

PL (dBm) = model or signal generated reception level for outdoor environment.

PL (d_0) = path loss within the antenna at the distance i.e 100 square meters around the transmitters (base station).

U = the loss constant, which is also known as the path loss exponent, which varies with the distance and mathematically represented as;

$$U = Y = \frac{p_m}{p_c}$$ 3.7

P_m = mean of the measured signal strength

P_c = mean of the calculated signal strength

3.11. Calculation Of Y (modeled loss constant) For Each Of The Locations For The Research Period.

3.11.1. College Of Medicine Aau, Ekpoma Location

Table 3.34: For The Month Of October, 2012

d (km)	p_c (dBm)	p_m (dBm)	$u = y = p_m/p_c$
1.00	-40.10	-75.70	1.89
2.00	-52.10	-77.90	1.50
3.00	-59.20	-81.40	1.38
4.00	-64.20	-81.50	1.27
5.00	-68.00	-78.80	1.16

Table 3.35: For The Month Of November, 2012

d (km)	p_c (dBm)	p_m (dBm)	u = y = p_m/p_c
1.00	-40.10	-78.80	2.01
2.00	-52.10	-73.40	1.53
3.00	-59.20	-76.90	1.30
4.00	-64.20	-75.10	1.31
5.00	-68.00	-77.10	1.20

Table 3.36: For The Month Of December, 2012

d (km)	p_c (dBm)	p_m (dBm)	u = y = p_m/p_c
1.00	-40.10	-77.00	1.92
2.00	-52.10	-81.40	1.56
3.00	-59.20	-89.00	1.50
4.00	-64.20	-76.50	1.20
5.00	-68.00	-75.00	1.10

Table 3.37: For The Month Of January, 2013

d (km)	p_c (dBm)	p_m (dBm)	u = y = p_m/p_c
1.00	-40.10	-85.00	2.14
2.00	-52.10	-79.20	1.52
3.00	-59.20	-79.50	1.34
4.00	-64.20	-78.20	1.22
5.00	-68.00	-79.10	1.16

Table 3.38: For The Month Of February, 2013

d (km)	p_c (dBm)	p_m (dBm)	u = y = p_m/p_c
1.00	-40.10	-80.40	2.00
2.00	-52.10	-82.60	1.59
3.00	-59.20	-83.40	1.41
4.00	-64.20	-82.90	1.29
5.00	-68.00	-85.80	1.26

Table 3.39: For The Month Of March, 2013

d (km)	p_c (dBm)	p_m (dBm)	u = y = p_m/p_c
1.00	-40.10	-84.30	2.10
2.00	-52.10	-80.30	1.54
3.00	-59.20	-84.40	1.43
4.00	-64.20	-83.40	1.30
5.00	-68.00	-86.60	1.27

3.11.2. Ujoelen, Ekpoma Location

Table 3.40: For The Month Of October, 2012

d (km)	p_c (dBm)	p_m (dBm)	$u = y = p_m/p_c$
1.00	-40.10	-73.80	1.84
2.00	-52.10	-73.40	1.41
3.00	-59.20	-76.40	1.30
4.00	-64.20	-75.00	1.27
5.00	-68.00	-77.70	1.14

Table 3.41: For The Month Of November, 2012

d (km)	p_c (dBm)	p_m (dBm)	$u = y = p_m/p_c$
1.00	-40.10	-71.20	1.80
2.00	-52.10	-69.00	1.30
3.00	-59.20	-67.00	1.13
4.00	-64.20	-71.70	1.12
5.00	-68.00	-71.00	1.04

Table 3.42: For The Month Of December, 2012

d (km)	p_c (dBm)	p_m (dBm)	$u = y = p_m/p_c$
1.00	-40.10	-74.20	1.85
2.00	-52.10	-75.60	1.45
3.00	-59.20	-75.80	1.30
4.00	-64.20	-76.50	1.19
5.00	-68.00	-74.80	1.10

Table 3.43: For The Month Of January, 2013

d (km)	p_c (dBm)	p_m (dBm)	$u = y = p_m/p_c$
1.00	-40.10	-75.60	1.89
2.00	-52.10	-72.20	1.39
3.00	-59.20	-73.90	1.25
4.00	-64.20	-69.60	1.08
5.00	-68.00	-78.50	1.15

Table 3.44: For The Month Of February, 2013

d (km)	p_c (dBm)	p_m (dBm)	$u = y = p_m/p_c$
1.00	-40.10	-72.40	1.81
2.00	-52.10	-75.90	1.46
3.00	-59.20	-71.90	1.21
4.00	-64.20	-74.30	1.26
5.00	-68.00	-76.40	1.12

Table 3.45: For The Month Of March, 2013

d (km)	p_c (dBm)	p_m (dBm)	$u = y = p_m/p_c$
1.00	-40.10	-73.30	1.83
2.00	-52.10	-69.50	1.33
3.00	-59.20	-73.10	1.23
4.00	-64.20	-73.30	1.14
5.00	-68.00	-75.00	1.10

3.11.3. For Eguare, Ekpoma Location

Table 3.46: For The Month Of October, 2012

d (km)	p_c (dBm)	p_m (dBm)	$u = y = p_m/p_c$
1.00	-40.10	-61.00	1.52
2.00	-52.10	-56.90	1.09
3.00	-59.20	-60.10	1.02
4.00	-64.20	-60.20	0.94
5.00	-68.00	-55.40	0.81

Table 3.47: For The Month Of November, 2012

d (km)	p_c (dBm)	p_m (dBm)	$u = y = p_m/p_c$
1.00	-40.10	-59.00	1.47
2.00	-52.10	-57.70	1.11
3.00	-59.20	-57.80	0.98
4.00	-64.20	-60.20	0.94
5.00	-68.00	-58.20	0.86

Table 3.48: For The Month Of December, 2012

d (km)	p_c (dBm)	p_m (dBm)	$u = y = p_m/p_c$
1.00	-40.10	-60.50	1.51
2.00	-52.10	-59.40	1.14
3.00	-59.20	-58.90	0.99
4.00	-64.20	-59.30	0.92
5.00	-68.00	-62.10	0.91

Table 3.49: For The Month Of January, 2013

d (km)	p_c (dBm)	p_m (dBm)	$u = y = p_m/p_c$
1.00	-40.10	-60.40	1.51
2.00	-52.10	-58.50	1.12
3.00	-59.20	-60.50	1.02
4.00	-64.20	-61.20	0.95
5.00	-68.00	-62.90	0.93

Table 3.50: For The Month Of February, 2013

d (km)	p_c (dBm)	p_m (dBm)	$u = y = p_m/p_c$
1.00	-40.10	-56.80	1.42
2.00	-52.10	-58.80	1.13
3.00	-59.20	-62.90	1.06
4.00	-64.20	-59.40	0.93
5.00	-68.00	-61.80	0.91

Table 3.51: For The Month Of March, 2012

d (km)	p_c (dBm)	p_m (dBm)	$u = y = p_m/p_c$
1.00	-40.10	-64.50	1.61
2.00	-52.10	-60.60	1.16
3.00	-59.20	-61.30	1.04
4.00	-64.20	-59.50	0.93
5.00	-68.00	-61.80	0.91

3.11.4. Emuado Campus Aau, Ekpoma Location

Table 3.52: For The Month Of October, 2012

d (km)	p_c (dBm)	p_m (dBm)	$u = y = p_m/p_c$
1.00	-40.10	-77.30	1.93
2.00	-52.10	-77.60	1.49
3.00	-59.20	-78.60	1.33
4.00	-64.20	-80.00	1.25
5.00	-68.00	-80.90	1.19

Table 3.53: For The Month Of November, 2012

d (km)	p_c (dBm)	p_m (dBm)	$u = y = p_m/p_c$
1.00	-40.10	-79.20	1.98
2.00	-52.10	-77.80	1.49
3.00	-59.20	-81.60	1.38
4.00	-64.20	-75.70	1.18
5.00	-68.00	-76.90	1.13

Table 3.54: For The Month Of December, 2012

d (km)	p_c (dBm)	p_m (dBm)	$u = y = p_m/p_c$
1.00	-40.10	-80.50	2.01
2.00	-52.10	-81.30	1.56
3.00	-59.20	-83.20	1.41
4.00	-64.20	-81.50	1.27
5.00	-68.00	-85.10	1.25

Table 3.55: For The Month Of January, 2013

d (km)	p_c (dBm)	p_m (dBm)	$u = y = p_m/p_c$
1.00	-40.10	-80.80	2.01
2.00	-52.10	-82.90	1.59
3.00	-59.20	-82.50	1.39
4.00	-64.20	-80.90	1.26
5.00	-68.00	-82.50	1.21

Table 3.56: For The Month Of February, 2013

d (km)	p_c (dBm)	p_m (dBm)	$u = y = p_m/p_c$
1.00	-40.10	-79.10	1.97
2.00	-52.10	-82.80	1.59
3.00	-59.20	-82.90	1.40
4.00	-64.20	-83.90	1.31
5.00	-68.00	-85.30	1.25

Table 3.57: For The Month Of March, 2013

d (km)	p_c (dBm)	p_m (dBm)	$u = y = p_m/p_c$
1.00	-40.10	-85.40	2.13
2.00	-52.10	-83.20	1.60
3.00	-59.20	-84.80	1.43
4.00	-64.20	-84.10	1.31
5.00	-68.00	-83.90	1.23

3.12. Calculation Of Signal Using Uzairue's Generated Model And Generated Loss Constant.

$$PL(dBm) = PL(do) + U10n\log\frac{d_i}{d_0}$$
$$4.8$$

And the loss constant for each of the locations for the period tested has been calculated from Table 3.34 to 3.57.

Recall that, PL (d_0) = 0.0775 (which was gotten from this equation

$$PL(dB) = -10\log\frac{\lambda^2}{(4\pi)^2 d^2}.)$$

d_i = variable distance of the base station

d_0 = fixed or reference distance

$n = \dfrac{3+5}{2}$ = 4 (mean of the path loss exponent of a shadow urban environment) and U = Y has been calculated which is the generated loss constant.

3.12.1. College Of Medicine Campus, AAU, Ekpoma Location
Table 3.58: For The Month Of October, 2012

d (km)	d/d$_0$	logd/d$_0$	Y	Y10n	Y10nlog(d/d$_0$)	PL(dBm) = PL(d$_0$)+Y10nlog(d/d$_0$)
1.00	10.00	1.00	1.89	75.60	75.60	-75.60
2.00	20.00	1.30	1.50	60.00	78.00	-78.00
3.00	30.00	1.48	1.38	55.20	81.70	-81.70
4.00	40.00	1.60	1.27	50.80	81.30	-80.30
5.00	50.00	1.69	1.16	46.40	78.40	-78.40

n = 4
10n = 40

$d_0 = 100m$

$PL(d_0) = 0.0775$

Table 3.59: For The Month Of November, 2012

d (km)	d/d₀	logd/d₀	Y	Y10n	Y10nlog(d/d₀)	PL(dBm) = PL(d₀)+Y10nlog(d/d₀)
1.00	10.00	1.00	2.01	80.40	80.40	-80.50
2.00	20.00	1.30	1.53	61.20	79.56	-79.60
3.00	30.00	1.48	1.34	53.60	79.30	-79.40
4.00	40.00	1.60	1.31	52.40	83.80	-84.00
5.00	50.00	1.69	1.20	48.00	81.10	-81.20

n = 4

10n = 40

$d_0 = 100m$

PL (d0) = 0.0775

Table 3.60: For The Month Of December, 2012

d (km)	d/d₀	logd/d₀	Y	Y10n	Y10nlog(d/d₀)	PL(dBm) = PL(d₀)+Y10nlog(d/d₀)
1.00	10.00	1.00	1.92	76.80	76.80	-76.90
2.00	20.00	1.30	1.56	62.40	81.10	-81.20
3.00	30.00	1.48	1.50	60.00	88.80	-88.90
4.00	40.00	1.60	1.20	48.00	76.80	-76.90
5.00	50.00	1.69	1.10	44.00	74.40	-74.43

n = 4

10n = 40

$d_0 = 100m$

$PL(d_0) = 0.0775$

Table 3.61: For The Month Of January, 2013

d (km)	d/d₀	logd/d₀	Y	Y10n	Y10nlog(d/d₀)	PL(dBm) = PL(d₀)+Y10nlog(d/d₀)
1.00	10.00	1.00	2.14	85.60	85.60	-85.70
2.00	20.00	1.30	1.52	60.80	79.04	-79.12
3.00	30.00	1.48	1.34	53.60	79.33	-79.41
4.00	40.00	1.60	1.22	48.80	78.08	-78.30
5.00	50.00	1.69	1.16	46.40	78.42	-79.49

n = 4

10n = 40

$d_0 = 100m$

$PL(d_0) = 0.0775$

Table 3.62: For The Month Of February, 2012

d (km)	d/d_0	$\log d/d_0$	Y	Y10n	$Y10n\log(d/d_0)$	PL(dBm) = $PL(d_0)+Y10n\log(d/d_0)$
1.00	10.00	1.00	2.00	80.00	80.00	-80.10
2.00	20.00	1.30	1.59	63.60	82.70	-72.80
3.00	30.00	1.48	1.41	56.40	83.50	-83.50
4.00	40.00	1.60	1.29	51.60	82.56	-82.70
5.00	50.00	1.69	1.26	50.40	85.16	-85.21

n = 4
10n = 40
d_0 = 100m
PL (d_0) = 0.0775

Table 3.63: For The Month Of March, 2013

d (km)	d/d_0	$\log d/d_0$	Y	Y10n	$Y10n\log(d/d_0)$	PL(dBm) = $PL(d_0)+Y10n\log(d/d_0)$
1.00	10.00	1.00	2.10	84.00	84.00	-84.10
2.00	20.00	1.30	1.54	61.60	80.08	-80.15
3.00	30.00	1.48	1.43	57.20	84.75	-84.73
4.00	40.00	1.60	1.30	52.00	83.20	-83.40
5.00	50.00	1.69	1.27	50.80	85.85	-86.92

n = 4
10n = 40
d_0 = 100m
PL (d_0) = 0.0775

3.12.2. Ujoelen, Ekpoma Location

Table 3.64 For The Month Of October, 2012

d	d/d_0	$\log d/d_0$	Y	Y10n	$Y10n\log(d/d_0)$	PL(dBm) = $PL(d_0)+Y10n\log(d/d_0)$
1.00	10.00	1.00	1.84	73.60	73.60	-73.70
2.00	20.00	1.30	1.41	56.40	73.30	-73.50
3.00	30.00	1.48	1.30	52.00	56.96	-84.73
4.00	40.00	1.60	1.17	46.80	74.88	-75.10
5.00	50.00	1.69	1.14	45.60	77.06	-77.60

n = 4
10n = 40
d_0 = 100m
PL (d_0) = 0.0775

Table 3.65: For The Month Of November, 2012

d	d/d_0	$\log d/d_0$	Y	Y10n	Y10nlog(d/d_0)	PL(dBm) = PL(d_0)+Y10nlog(d/d_0)
1.00	10.00	1.00	1.80	72.00	72.00	-72.10
2.00	20.00	1.30	1.30	52.00	67.60	-67.70
3.00	30.00	1.48	1.13	45.20	66.89	-66.97
4.00	40.00	1.60	1.12	44.80	71.68	-71.80
5.00	50.00	1.69	1.04	41.60	70.30	-70.38

n = 4
10n = 40
d_0 = 100m
PL (d_0) = 0.0775

Table 3.66: For The Month Of December, 2012

d (km)	d/d_0	$\log d/d_0$	Y	Y10n	Y10nlog(d/d_0)	PL(dBm) = PL(d_0)+Y10nlog(d/d_0)
1.00	10.00	1.00	1.85	74.00	74.00	-74.10
2.00	20.00	1.30	1.45	58.00	75.40	-75.50
3.00	30.00	1.48	1.30	52.00	76.96	-77.03
4.00	40.00	1.60	1.19	47.60	76.16	-76.30
5.00	50.00	1.69	1.10	44.00	74.36	-74.80

n = 4
10n = 40
d_0 = 100m
PL (d_0) = 0.0775

Table 3.67: For The Month Of January, 2013

d (km)	d/d0	$\log d/d_0$	Y	Y10n	Y10nlog(d/d_0)	PL(dBm) = PL(d_0)+Y10nlog(d/d_0)
1.00	10.00	1.00	1.89	75.60	75.60	-75.70
2.00	20.00	1.30	1.39	55.60	72.28	-72.40
3.00	30.00	1.48	1.25	50.00	74.00	-74.07
4.00	40.00	1.60	1.08	43.20	69.12	-69.30
5.00	50.00	1.69	1.15	46.00	77.74	-78.20

n = 4
10n = 40
d_0 = 100m
PL (d_0) = 0.0775

Table 3.68: For The Month Of February, 2013

d (km)	d/d_0	$\log d/d_0$	Y	Y10n	$Y10n\log(d/d_0)$	PL(dBm) = $PL(d_0)+Y10n\log(d/d_0)$
1.00	10.00	1.00	1.81	72.40	72.40	-72.50
2.00	20.00	1.30	1.46	58.40	75.92	-76.10
3.00	30.00	1.48	1.21	48.40	71.63	-71.70
4.00	40.00	1.60	1.16	46.40	74.24	-74.40
5.00	50.00	1.69	1.12	44.80	75.71	-76.20

n = 4

10n = 40

d_0 = 100m

PL (d_0) = 0.0775

Table 3.69: For The Month Of March, 2013

d (km)	d/d_0	$\log d/d_0$	Y	Y10n	$Y10n\log(d/d_0)$	PL(dBm) = $PL(d_0)+Y10n\log(d/d_0)$
1.00	10.00	1.00	1.83	73.20	73.20	-73.30
2.00	20.00	1.30	1.33	53.20	69.16	-69.29
3.00	30.00	1.48	1.25	50.00	74.00	-74.08
4.00	40.00	1.60	1.14	45.60	72.96	-73.10
5.00	50.00	1.69	1.10	44.00	74.36	-74.43

n = 4

10n = 40

d_0 = 100m

PL (d_0) = 0.0775

3.12.3. Eguare Ekpoma Location

Table 3.70: For The Month Of October, 2012

d (km)	d/d_0	$\log d/d_0$	Y	Y10n	$Y10n\log(d/d_0)$	PL(dBm) = $PL(d_0)+Y10n\log(d/d_0)$
1.00	10.00	1.00	1.52	60.80	60.80	-60.87
2.00	20.00	1.30	1.09	43.60	56.68	-56.76
3.00	30.00	1.48	1.02	40.80	60.38	-60.46
4.00	40.00	1.60	0.92	36.80	58.88	-58.96
5.00	50.00	1.69	0.82	32.80	55.43	-55.51

n = 4

10n = 40

d_0 = 100m

PL (d_0) = 0.0775

Table 3.71: For The Month Of November, 2012

d (km)	d/d_0	$\log d/d_0$	Y	Y10n	$Y10n\log(d/d_0)$	PL(dBm) = $PL(d_0)+Y10n\log(d/d_0)$
1.00	10.00	1.00	1.47	58.80	58.80	-58.87
2.00	20.00	1.30	1.11	44.40	57.72	-57.79
3.00	30.00	1.48	0.98	39.20	58.02	-58.09
4.00	40.00	1.60	0.94	37.60	60.16	-60.24
5.00	50.00	1.69	0.86	37.40	58.14	-58.21

n = 4
10n = 40
d_0 = 100m
PL (d_0) = 0.0775

Table 3.72: For The Month Of December, 2012

d (km)	d/d_0	$\log d/d_0$	Y	Y10n	$Y10n\log(d/d_0)$	PL(dBm) = $PL(d_0)+Y10n\log(d/d_0)$
1.00	10.00	1.00	1.51	60.40	60.40	-60.47
2.00	20.00	1.30	1.14	45.60	59.28	-59.36
3.00	30.00	1.48	0.99	39.60	58.61	58.69
4.00	40.00	1.60	0.92	36.80	58.88	-58.96
5.00	50.00	1.69	0.91	36.40	61.52	-61.59

n = 4
10n = 40
d_0 = 100m
PL (d_0) = 0.0775

Table 3.73: For The Month Of January, 2013

d (km)	d/d_0	$\log d/d_0$	Y	Y10n	$Y10n\log(d/d_0)$	PL(dBm) = $PL(d_0)+Y10n\log(d/d_0)$
1.00	10.00	1.00	1.51	60.40	60.40	-60.47
2.00	20.00	1.30	1.12	44.80	58.24	-58.32
3.00	30.00	1.48	1.02	40.80	60.38	-60.46
4.00	40.00	1.60	0.95	38.00	60.80	-60.88
5.00	50.00	1.69	0.93	37.20	62.87	-62.95

n = 4
10n = 40
d_0 = 100m
PL (d_0) = 0.0775

Table 3.74: For The Month Of February, 2013

d (km)	d/d_0	$\log d/d_0$	Y	Y10n	Y10nlog(d/d_0)	PL(dBm) = $PL(d_0)+Y10n\log(d/d_0)$
1.00	10.00	1.00	1.42	56.80	56.80	-56.87
2.00	20.00	1.30	1.13	45.20	58.76	-58.84
3.00	30.00	1.48	1.06	42.40	62.74	-62.83
4.00	40.00	1.60	0.93	37.20	59.52	-59.59
5.00	50.00	1.69	0.91	36.40	61.52	-61.59

n = 4

10n = 40

d_0 = 100m

PL (d_0) = 0.0775

Table 3.75: For The Month Of March, 2013

d (km)	d/d_0	$\log d/d_0$	Y	Y10n	Y10nlog(d/d_0)	PL(dBm) = $PL(d_0)+Y10n\log(d/d_0)$
1.00	10.00	1.00	1.61	64.40	64.40	-64.47
2.00	20.00	1.30	1.16	46.40	60.32	-60.39
3.00	30.00	1.48	1.04	41.60	61.57	-61.65
4.00	40.00	1.60	0.93	37.20	59.52	-61.65
5.00	50.00	1.69	0.91	36.40	61.52	-61.59

n = 4

10n = 40

d_0 = 100m

PL (d_0) = 0.0775

3.12.4. Emuado Campus, AAU Ekpoma

Table 3.76: For The Month Of October, 2012

d (km)	d/d_0	$\log d/d_0$	Y	Y10n	Y10nlog(d/d_0)	PL(dBm) = $PL(d_0)+Y10n\log(d/d_0)$
1.00	10.00	1.00	1.93	77.20	77.20	-77.27
2.00	20.00	1.30	1.49	59.60	77.48	-77.56
3.00	30.00	1.48	1.33	53.20	78.74	-78.81
4.00	40.00	1.60	1.25	50.00	80.00	-80.07
5.00	50.00	1.69	1.19	47.60	80.44	-80.52

n = 4

10n = 40

d_0 = 100m

PL (d_0) = 0.0775

Table 3.77: For The Month Of November, 2012

d (km)	d/d_0	$\log d/d_0$	Y	Y10n	Y10nlog(d/d_0)	PL(dBm) = PL(d_0)+Y10nlog(d/d_0)
1.00	10.00	1.00	2.01	80.40	80.40	-80.47
2.00	20.00	1.30	1.56	62.40	81.12	-81.19
3.00	30.00	1.48	1.41	56.40	83.47	-83.55
4.00	40.00	1.60	1.27	50.80	81.28	-81.36
5.00	50.00	1.69	1.25	50.00	84.50	-84.57

n = 4
10n = 40
d_0 = 100m
PL (d_0) = 0.0775

Table 3.78: For The Month Of January, 2013

d (km)	d/d_0	$\log d/d_0$	Y	Y10n	Y10nlog(d/d_0)	PL(dBm) = PL(d_0)+Y10nlog(d/d_0)
1.00	10.00	1.00	2.01	80.40	80.40	-80.47
2.00	20.00	1.30	1.59	63.60	82.68	-82.76
3.00	30.00	1.48	1.39	55.60	82.29	-82.37
4.00	40.00	1.60	1.26	50.40	80.64	-80.72
5.00	50.00	1.69	1.21	48.40	81.79	-81.87

n = 4
10n = 40
d_0 = 100m
PL (d_0) = 0.0775

Table 3.79: For The Month Of February, 2013

d (km)	d/d_0	$\log d/d_0$	Y	Y10n	Y10nlog(d/d_0)	PL(dBm) = PL(d_0)+Y10nlog(d/d_0)
1.00	10.00	1.00	1.97	78.80	78.80	-78.87
2.00	20.00	1.30	1.59	63.60	82.68	-82.76
3.00	30.00	1.48	1.40	56.00	82.88	-82.96
4.00	40.00	1.60	1.31	52.40	83.84	-83.92
5.00	50.00	1.69	1.25	50.00	84.50	84.57

n = 4
10n = 40
d_0 = 100m
PL (d_0) = 0.0775

Table 3.80: For The Month Of March, 2013

d (km)	d/d$_0$	logd/d$_0$	Y	Y10n	Y10nlog(d/d$_0$)	PL(dBm) = PL(d$_0$)+Y10nlog(d/d$_0$)
1.00	10.00	1.00	2.13	85.20	85.20	-85.27
2.00	20.00	1.30	1.50	60.00	78.00	-78.07
3.00	30.00	1.48	1.43	57.20	84.65	-84.73
4.00	40.00	1.60	1.31	52.40	83.83	-83.92
5.00	50.00	1.69	1.23	49.20	83.15	-83.23

n = 4

10n = 40

d$_0$ = 100m

PL (d$_0$) = 0.0775

3.13. Calculation Of Path Loss Exponent For The Different Locations

In finding the path loss exponent for the different locations, the mean or average of the loss constant at different distance (1km, 2km, 3km, 4km and 5km) for the locations used was put into consideration.

3.13.1. Calculation Of The Path Loss Exponent For College Of Medicine

For The Month Of October, 2012.

$$n = \frac{1.89 + 1.50 + 1.38 + 1.27 + 1.16}{5}$$

= 1.44

For The Month Of November, 2012.

$$n = \frac{2.01 + 1.53 + 1.34 + 1.31 + 1.20}{5}$$

= 1.48

For The Month Of December, 2012.

$$n = \frac{1.92 + 1.56 + 1.50 + 1.20 + 1.10}{5}$$

= 1.46

For The Month Of January, 2013.

$$n = \frac{2.14 + 1.52 + 1.34 + 1.22 + 1.16}{5}$$

= 1.48

For The Month Of February, 2013.

$$n = \frac{2.00 + 1.59 + 1.41 + 1.29 + 1.26}{5}$$

= 1.51

For The Month Of March, 2013.

$$n = \frac{2.10 + 1.54 + 1.43 + 1.30 + 1.27}{5}$$

= 1.53

3.13.2. Calculation Of The Path Loss Exponent For Ujoelen Ekpoma

For The Month Of October, 2012.

$$n = \frac{1.84 + 1.41 + 1.30 + 1.17 + 1.14}{5}$$

= 1.37

For The Month Of November, 2012.

$$n = \frac{1.80 + 1.30 + 1.13 + 1.12 + 1.04}{5}$$

= 1.28

For The Month Of December, 2012.

$$n = \frac{1.85 + 1.45 + 1.30 + 1.19 + 1.10}{5}$$

= 1.38

For The Month Of January, 2013.

$$n = \frac{1.89 + 1.39 + 1.25 + 1.08 + 1.15}{5}$$

= 1.35

For The Month Of February, 2013.

$$n = \frac{1.81 + 1.46 + 1.21 + 1.16 + 1.12}{5}$$

= 1.35

For The Month Of March, 2013.

$$n = \frac{1.83 + 1.33 + 1.23 + 1.14 + 1.10}{5}$$

= 1.33

3.13.3. Calculation Of The Path Loss Exponent For Eguare Ekpoma

For The Month Of October, 2012.

$$n = \frac{1.52 + 1.09 + 1.50 + 0.94 + 0.81}{5}$$

= 1.17

For The Month Of November, 2012.

$$n = \frac{1.47 + 1.11 + 0.98 + 0.94 + 0.86}{5}$$

= 1.07

For The Month Of December, 2012.

$$n = \frac{1.51 + 1.14 + 0.99 + 0.92 + 0.91}{5}$$

   = 1.09

For The Month Of January, 2013.

$$n = \frac{1.51 + 1.12 + 1.02 + 0.95 + 0.93}{5}$$

   = 1.11

For The Month Of February, 2013.

$$n = \frac{1.42 + 1.13 + 1.06 + 0.93 + 0.91}{5}$$

   = 1.09

For The Month Of March, 2013.

$$n = \frac{1.61 + 1.16 + 1.04 + 0.93 + 0.91}{5}$$

   = 1.13

3.13.4. Calculation Of The Path Loss Exponent For Emaudo Campus

For The Month Of October, 2012.

$$n = \frac{1.93 + 1.49 + 1.33 + 1.25 + 1.19}{5}$$

= 1.43

For The Month Of November, 2012.

$$n = \frac{1.98 + 1.49 + 1.38 + 1.18 + 1.13}{5}$$

= 1.43

For The Month Of December, 2012.

$$n = \frac{2.01 + 1.56 + 1.41 + 1.27 + 1.25}{5}$$

= 1.50

For The Month Of January, 2013.

$$n = \frac{2.01 + 1.59 + 1.39 + 1.26 + 1.21}{5}$$

= 1.50

For The Month Of February, 2013.

$$n = \frac{1.97 + 1.59 + 1.40 + 1.31 + 1.25}{5}$$

= 1.50

For The Month Of March, 2013.

$$n = \frac{2.13 + 1.60 + 1.43 + 1.31 + 1.23}{5}$$

= 1.54

CHAPTER FOUR

RESULTS AND DISCUSSION

4.1. Results

4.1.1. Table 4.1 – 4.24: Shows The Summary Of The Comparison Between Path Loss Values From Measurement and Using Model Equation.

4.1.1.1. For College of Medicine, AAU, Ekpoma

Table 4.1: College Of Medicine For The Month Of October, 2012.

Distance km	PL (dBm) From Equation	PL (dBm) From Measurement.
1	-40.1	-75.7
2	-52.1	-77.9
3	-59.2	-81.4
4	-64.2	-81.5
5	-68.0	-78.8

Table 4.2: College Of Medicine For The Month Of November, 2012.

Distance km	PL (dBm) From Equation	PL (dBm) From Measurement.
1	-40.1	-80.8
2	-52.1	-79.7
3	-59.2	-79.6
4	-64.2	-83.8
5	-68.0	-79.8

Table 4.3: College Of Medicine For The Month Of December, 2012.

Distance km	PL (dBm) From Equation	PL (dBm) From Measurement.
1	-40.1	-77.0
2	-52.1	-81.4
3	-59.2	-89.0
4	-64.2	-76.5
5	-68.0	-75.0

Table 4.4: College Of Medicine For The Month Of January, 2013.

Distance km	PL (dBm) From Equation	PL (dBm) From Measurement.
1	-40.1	-85.9
2	-52.1	-79.2
3	-59.2	-79.5
4	-64.2	-78.2
5	-68.0	-79.1

Table 4.5: College Of Medicine For The Month Of February, 2013.

Distance km	PL (dBm) From Equation	PL (dBm) From Measurement.
1	-40.1	-80.4
2	-52.1	-82.6
3	-59.2	-83.4
4	-64.2	-82.9
5	-68.0	-85.8

Table 4.6: College Of Medicine For The Month Of March, 2013.

Distance km	PL (dBm) From Equation	PL (dBm) From Measurement.
1	-40.1	-84.3
2	-52.1	-80.8
3	-59.2	-84.4
4	-64.2	-83.4
5	-68.0	-86.6

4.1.1.2. For Ujoelen, Ekpoma Location

Table 4.7: Ujoelen For The Month Of October, 2012.

Distance km	PL (dBm) From Equation	PL (dBm) From Measurement.
1	-40.1	-73.8
2	-52.1	-73.4
3	-59.2	-76.9
4	-64.2	-75.0
5	-68.0	-77.7

Table 4.8: Ujoelen For The Month Of November, 2012.

Distance km	PL (dBm) From Equation	PL (dBm) From Measurement.
1	-40.1	-71.2
2	-52.1	-69.0
3	-59.2	-67.0
4	-64.2	-71.7
5	-68.0	-71.0

Table 4.9: Ujoelen For The Month Of December, 2012.

Distance km	PL (dBm) From Equation	PL (dBm) From Measurement.
1	-40.1	-74.2
2	-52.1	-75.6
3	-59.2	-75.8
4	-64.2	-76.5
5	-68.0	-74.8

Table 4.10: Ujoelen For The Month Of January, 2013.

Distance km	PL (dBm) From Equation	PL (dBm) From Measurement.
1	-40.1	-75.6
2	-52.1	-72.2
3	-59.2	-73.9
4	-64.2	-69.6
5	-68.0	-78.5

Table 4.11: Ujoelen For The Month Of February, 2013.

Distance km	PL (dBm) From Equation	PL (dBm) From Measurement.
1	-40.1	-72.4
2	-52.1	-75.9
3	-59.2	-71.9
4	-64.2	-74.3
5	-68.0	-76.4

Table 4.12: Ujoelen For The Month Of March, 2013.

Distance km	PL (dBm) From Equation	PL (dBm) From Measurement.
1	-40.1	-73.3
2	-52.1	-69.5
3	-59.2	-73.1
4	-64.2	-73.3
5	-68.0	-75.0

4.1.1.3. For Eguare Location

Table 4.13: Eguare, Ekpoma For The Month Of October, 2012.

Distance km	PL (dBm) From Equation	PL (dBm) From Measurement.
1	-40.1	-61.0
2	-52.1	-56.9
3	-59.2	-60.1
4	-64.2	-60.2
5	-68.0	-55.4

Table 4.14: Eguare, Ekpoma For The Month Of November, 2012.

Distance km	PL (dBm) From Equation	PL (dBm) From Measurement.
1	-40.1	-59.0
2	-52.1	-57.7
3	-59.2	-57.8
4	-64.2	-60.2
5	-68.0	-58.4

Table 4.15: Eguare, Ekpoma For The Month Of December, 2012.

Distance km	PL (dBm) From Equation	PL (dBm) From Measurement.
1	-40.1	-60.5
2	-52.1	-59.4
3	-59.2	-58.9
4	-64.2	-59.3
5	-68.0	-62.1

Table 4.16: Eguare, Ekpoma For The Month Of January, 2013.

Distance km	PL (dBm) From Equation	PL (dBm) From Measurement.
1	-40.1	-60.4
2	-52.1	-58.5
3	-59.2	-60.5
4	-64.2	-61.2
5	-68.0	-62.9

Table 4.17: Eguare, Ekpoma For The Month Of February, 2013.

Distance km	PL (dBm) From Equation	PL (dBm) From Measurement.
1	-40.1	-56.8
2	-52.1	-58.8
3	-59.2	-62.9
4	-64.2	-59.4
5	-68.0	-61.8

Table 4.18: Eguare, Ekpoma For The Month Of March, 2013.

Distance km	PL (dBm) From Equation	PL (dBm) From Measurement.
1	-40.1	-64.5
2	-52.1	-60.6
3	-59.2	-61.3
4	-64.2	-59/5
5	-68.0	-61.8

4.1.1.4. Emaudo Campus, AAU, Ekpoma

Table 4.19: Emaudo Campus, A.A.U, Ekpoma For The Month Of October, 2012.

Distance km	PL (dBm) From Equation	PL (dBm) From Measurement.
1	-40.1	-77.3
2	-52.1	-77.6
3	-59.2	-78.6
4	-64.2	-80.0
5	-68.0	-80.9

Table 4.20: Emaudo Campus, A.A.U, Ekpoma For The Month Of November, 2012.

Distance km	PL (dBm) From Equation	PL (dBm) From Measurement.
1	-40.1	-79.2
2	-52.1	-77.8
3	-59.2	-81.6
4	-64.2	-75.7
5	-68.0	-76.9

Table 4.21: Emaudo Campus, A.A.U, Ekpoma For The Month Of December, 2012.

Distance km	PL (dBm) From Equation	PL (dBm) From Measurement.
1	-40.1	-80.5
2	-52.1	-81.3
3	-59.2	-83.2
4	-64.2	-81.5
5	-68.0	-85.1

Table 4.22: Emaudo Campus, A.A.U, Ekpoma For The Month Of January, 2013.

Distance km	PL (dBm) From Equation	PL (dBm) From Measurement.
1	-40.1	-80.8
2	-52.1	-82.9
3	-59.2	-82.5
4	-64.2	-80.9
5	-68.0	-82.5

Table 4.24: Emaudo Campus, A.A.U, Ekpoma For The Month Of February, 2013.

Distance km	PL (dBm) From Equation	PL (dBm) From Measurement.
1	-40.1	-79.1
2	-52.1	-82.8
3	-59.2	-89.9
4	-64.2	-83.9
5	-68.0	-85.3

Table 4.24: Emaudo Campus, A.A.U, Ekpoma For The Month Of March, 2013.

Distance km	PL (dBm) From Equation	PL (dBm) From Measurement.
1	-40.1	-85.4
2	-52.1	-83.2
3	-59.2	-84.8
4	-64.2	-84.1
5	-68.0	-83.9

4.1.2. Comparison Between The Path Loss Values From Measurement, Using Deterministic/Theoretical Model (log-distance path loss model) And The Generated Empirical Model (Anyasi's model) For The Period Used For College Of Medicine, AAU Ekpoma.

Table 4.25: College Of Medicine For The Month Of October, 2012.

Distance km	PL(dBm) From Measurement	PL(dBm) From Equation	PL(dBm) From Anyasi's model
1	-75.7	-40.1	-75.6
2	-77.9	-52.1	-78.0
3	-81.4	-59.2	-81.7
4	-81.5	-64.2	-81.3
5	-78.8	-68.0	-78.4

Table 4.26: College Of Medicine For The Month Of November, 2012.

Distance km	PL(dBm) From Measurement	PL(dBm) From Equation	PL(dBm) From Anyasi's model
1	-80.8	-40.1	-80.5
2	-79.7	-52.1	-79.7
3	-79.6	-59.2	-79.2
4	-83.8	-64.2	-84.0
5	-79.8	-68.0	-81.6

Table 4.27: College Of Medicine For The Month Of December, 2012.

Distance km	PL(dBm) From Measurement	PL(dBm) From Equation	PL(dBm) From Anyasi's model
1	-77.0	-40.1	-76.9
2	-81.4	-52.1	-81.3
3	-89.0	-59.2	-88.7
4	-76.5	-64.2	-80.0
5	-75.0	-68.0	-74.8

Table 4.28: College Of Medicine For The Month Of January, 2013.

Distance km	PL(dBm) From Measurement	PL(dBm) From Equation	PL(dBm) From Anyasi's model
1	-85.9	-40.1	-85.7
2	-79.2	-52.1	-79.2
3	-79.5	-59.2	-79.3
4	-78.2	-64.2	-78.3
5	-79.1	-68.0	-79.9

Table 4.29: College Of Medicine For The Month Of February, 2013.

Distance km	PL(dBm) From Measurement	PL(dBm) From Equation	PL(dBm) From Anyasi's model
1	-80.4	-40.1	-80.1
2	-82.6	-52.1	-82.8
3	-83.4	-59.2	-83.4
4	-82.9	-64.2	-82.7
5	-85.8	-68.0	-85.9

Table 4.30: College Of Medicine For The Month Of March, 2013.

Distance km	PL(dBm) From Measurement	PL(dBm) From Equation	PL(dBm) From Anyasi's model
1	-84.3	-40.1	-84.1
2	-80.8	-52.1	-80.2
3	-84.4	-59.2	-84.6
4	-83.4	-64.2	-83.4
5	-86.6	-68.0	-86.4

4.1.3. Comparison Between The Path Loss Values From Measurement, Using Deterministic/Theoretical Model (log-distance path loss model) And The Generated Empirical Model (Anyasi's model) For The Period Used ''Ujoelen Ekpoma''.

Table 4.31: Ujoelen, Ekpoma Location For The Month Of October, 2012

Distance km	PL(dBm) From Measurement	PL(dBm) From Equation	PL(dBm) From Anyasi's model
1	-73.8	-40.1	-73.7
2	-73.4	-52.1	-73.5
3	-76.9	-59.2	-76.9
4	-75.0	-64.2	-75.1
5	-77.7	-68.0	-77.6

Table 4.32: Ujoelen, Ekpoma Location For The Month Of November, 2012

Distance km	PL(dBm) From Measurement	PL(dBm) From Equation	PL(dBm) From Anyasi's model
1	-71.4	-40.1	-72.1
2	-69.0	-52.1	-67.7
3	-67.0	-59.2	-66.8
4	-71.7	-64.2	-71.8
5	-71.0	-68.0	-70.8

Table 4.33: Ujoelen, Ekpoma Location For The Month Of December, 2012

Distance km	PL(dBm) From Measurement	PL(dBm) From Equation	PL(dBm) From Anyasi's model
1	-74.2	-40.1	-74.1
2	-75.6	-52.1	-75.5
3	-75.8	-59.2	-76.9
4	-76.5	-64.2	-76.3
5	-74.8	-68.0	-74.8

Table 4.34: Ujoelen, Ekpoma Location For The Month Of January, 2013

Distance km	PL(dBm) From Measurement	PL(dBm) From Equation	PL(dBm) From Anyasi's model
1	-75.6	-40.1	-75.7
2	-72.2	-52.1	-72.4
3	-73.9	-59.2	-73.9
4	-69.6	-64.2	-69.3
5	-78.5	-68.0	-78.2

Table 4.35: Ujoelen, Ekpoma Location For The Month Of February, 2013

Distance km	PL(dBm) From Measurement	PL(dBm) From Equation	PL(dBm) From Anyasi's model
1	-72.4	-40.1	-72.5
2	-75.9	-52.1	-76.1
3	-71.9	-59.2	-71.6
4	-74.3	-64.2	-74.4
5	-76.4	-68.0	-76.2

Table 4.36: Ujoelen, Ekpoma Location For The Month Of March, 2012

Distance km	PL(dBm) From Measurement	PL(dBm) From Equation	PL(dBm) From Anyasi's model
1	-73.3	-40.1	-73.3
2	-69.5	-52.1	-69.3
3	-73.1	-59.2	-73.9
4	-73.3	-64.2	-73.1
5	-75.0	-68.0	-74.8

4.1.4. Comparison Between The Path Loss Values From Measurement, Using Deterministic/Theoretical Model (log-distance path loss model) And The Generated Empirical Model (Anyasi's model) For The Period Used ''Eguare Ekpoma''.

Table4.37: Eguare, Ekpoma Location For The Month Of October, 2012

Distance km	PL(dBm) From Measurement	PL(dBm) From Equation	PL(dBm) From Anyasi's model
1	-61.0	-40.1	-60.9
2	-56.9	-52.1	-56.8
3	-60.1	-59.2	-60.3
4	-60.2	-64.2	-60.3
5	-55.4	-68.0	-55.1

Table4.38: Eguare, Ekpoma Location For The Month Of November, 2012

Distance km	PL(dBm) From Measurement	PL(dBm) From Equation	PL(dBm) From Anyasi's model
1	-59.0	-40.1	-58.9
2	-57.7	-52.1	-57.8
3	-57.8	-59.2	-58.0
4	-60.2	-64.2	-60.3
5	-58.4	-68.0	-58.1

Table4.39: Eguare, Ekpoma Location For The Month Of December, 2012

Distance km	PL(dBm) From Measurement	PL(dBm) From Equation	PL(dBm) From Anyasi's model
1	-60.5	-40.1	-60.5
2	-59.4	-52.1	-59.4
3	-58.9	-59.2	-58.6
4	-59.3	-64.2	-59.0
5	-62.1	-68.0	-61.9

Table4.40: Eguare, Ekpoma Location For The Month Of January, 2013

Distance km	PL(dBm) From Measurement	PL(dBm) From Equation	PL(dBm) From Anyasi's model
1	-60.4	-40.1	-60.5
2	-58.5	-52.1	-58.4
3	-60.5	-59.2	-60.3
4	-61.2	-64.2	-61.0
5	-62.9	-68.0	-63.3

Table4.41: Eguare, Ekpoma Location For The Month Of February, 2013

Distance km	PL(dBm) From Measurement	PL(dBm) From Equation	PL(dBm) From Anyasi's model
1	-56.8	-40.1	-56.9
2	-58.8	-52.1	-56.9
3	-62.9	-59.2	-62.7
4	-59.4	-64.2	-59.7
5	-61.8	-68.0	-61.8

Table4.42: Eguare, Ekpoma Location For The Month Of March, 2013

Distance km	PL(dBm) From Measurement	PL(dBm) From Equation	PL(dBm) From Anyasi's model
1	-64.5	-40.1	-64.5
2	-60.5	-52.1	-60.4
3	-61.3	-59.2	-61.5
4	-59.5	-64.2	-59.7
5	-61.8	-68.0	-61.9

4.1.5. Comparison Between The Path Loss Values From Measurement, Using Deterministic/Theoretical Model (log-distance path loss model) And The Generated Empirical Model (Anyasi's model) For The Period Used ''Emaudo Ekpoma''.

Table 4.43: Emaudo Campus, AAU Location For The Month Of October, 2012

Distance km	PL(dBm) From Measurement	PL(dBm) From Equation	PL(dBm) From Anyasi's model
1	-77.3	-40.1	-77.3
2	-77.6	-52.1	-77.6
3	-78.6	-59.2	-78.7
4	-80.0	-64.2	-80.2
5	-80.9	-68.0	-80.9

Table 4.44: Emaudo Campus, AAU Location For The Month Of November, 2012

Distance km	PL(dBm) From Measurement	PL(dBm) From Equation	PL(dBm) From Anyasi's model
1	-79.2	-40.1	-79.3
2	-77.8	-52.1	-77.6
3	-81.6	-59.2	-81.6
4	-75.7	-64.2	-75.7
5	-76.9	-68.0	-76.9

Table 4.45: Emaudo Campus, AAU Location For The Month Of December, 2012

Distance km	PL(dBm) From Measurement	PL(dBm) From Equation	PL(dBm) From Anyasi's model
1	-80.5	-40.1	-80.5
2	-81.3	-52.1	-81.3
3	-83.2	-59.2	-83.4
4	-81.5	-64.2	-81.5
5	-85.1	-68.0	-85.0

Table 4.46: Emaudo Campus, AAU Location For The Month Of January, 2013

Distance km	PL(dBm) From Measurement	PL(dBm) From Equation	PL(dBm) From Anyasi's model
1	-80.8	-40.1	-80.5
2	-82.9	-52.1	-82.8
3	-82.5	-59.2	-82.2
4	-80.9	-64.2	-80.8
5	-82.5	-68.0	-82.3

Table 4.47: Emaudo Campus, AAU Location For The Month Of February, 2013.

Distance km	PL(dBm) From Measurement	PL(dBm) From Equation	PL(dBm) From Anyasi's model
1	-79.1	-40.1	-78.9
2	-82.8	-52.1	-82.8
3	-82.9	-59.2	-82.8
4	-83.9	-64.2	-84.0
5	-85.3	-68.0	-85.0

Table 4.48: Emaudo Campus, AAU Location For The Month Of March, 2012

Distance km	PL(dBm) From Measurement	PL(dBm) From Equation	PL(dBm) From Anyasi's model
1	-85.4	-40.1	-85.3
2	-83.2	-52.1	-78.1
3	-84.8	-59.2	-84.6
4	-84.1	-64.2	-91.7
5	-83.9	-68.0	-83.7

4.2. Results Discussion

From the Tables above, which shows the tables comparing the signal strength obtained from the existing model equation (log-distance equation), generated model equation and the one measured with RF

signal tracker, it was observed from the Tables that, the signal strength calculated from the existing equation was totally different from the one measured with the software (RF signal tracker) and the generated model equation in college of medicine, Ujoelen and Emaudo campus, was of large range difference and it was of lower values compare to the signal strength calculated with the existing equation but in the case of Eguare, it was observed that in all the months, between 4km to 5km the existing model equation was having lower values compared to the measured signal strength and generated model equation calculation. This could be as a result of the presence of trees, human population and traffic in that region.

CHAPTER FIVE

CONCLUSION AND RECOMMENDATION

5.1. Conclusion

The signal strength in the outdoor that was calculated from four different locations namely; College of medicine, AAU, Ekpoma, Emaudo campus, AAU Ekpoma, Ujoelen Ekpoma and Eguare Ekpoma were measured at the frequency range of 1800MHZ. Comparing the signal strength obtained from the generated model" Anyasi's model" and the measured signal strength obtained from RF signal tracker, it was observed that they are almost of the same values.

From the data, it was observed that the calculation of path loss with log – distance model which is deterministic is not as accurate as the empirical model (generated model), the generated model gave a better and more accurate result than the existing ones, and that the path loss exponents of the tested locations was fully known. Model was developed to calculate the power received of GSM signal in Ekpoma and the model was named after the researcher "Anyasi's model".

5.2. Contribution to Knowledge.

The contributions to knowledge of this research work are as follows;

1. It has provided the signal strength level for the tested locations (College of medicine AAU, Emaudo campus AAU, Ujoelen and Eguare).

2. It has provided an empirical model equation for the calculation of the outdoor propagation path loss in Ekpoma community.

3. It has provided the loss constant for Ekpoma community and the loss constant is very important to G.S.M industries.

4. It has shown that the empirical model generated (Anyasi's model) gives a better values than the existing ones, as shown from table 4.25 to 4.48.

5.3. Recommendation

For further research, the following recommendations are suggested:

1. Determining the relative error of signal strength in G.S.M networks.

   The formula for Relative Error is given as

   $$RE = \frac{PL(measured) - PL(predicted)}{PL(measured)}$$

2. Taking measurements at distance of 6 – 10km between receivers and transmitters.

REFERENCES

Ajakaye, T.A (2005) "Telecommunication Business in Nigeria" University of Lagos, Vol.1, pp. 37-51

Ajay Mishra (2007)"Advance Cellular Network Planning and Optimization" John Wiley and Sons, vol.28, pp.402-411.

Amitay, N. (1992) "*Modeling and Computer Simulation of Wave Propagation in Lineal Line-of Sight Microcell,*" IEEE Trans. Veh. Tech.; pp. 337-42.

Anderson, H. R. (2001) "*A Ray-Tracing Propagation Model for Digital Broadcast Systems in Urban Area,*" IEEE Trans. Broadcasting, vol. 39, pp. 309-317.

Andrea Goldsmiths (2005) "*Wireless Communications,*" Cambridge University Press, vol. 7, pp. 43-67

Andrea, G. (2005)"*Wireless communications,*" Cambridge University Press.

Armoogum.V, Soyjaudah.K.M.S, Fogarty T. and MohamudallyN. (2007) "Comparative study of Path loss using existing models for Digital Television Broadcasting for Summer, Mauritius Vol. 4, pp 34-38,May Season in the north of

Mauritius", Proceeding of Third Advanced IEEE International Conference on Telecommunication.

Arne Schmitz and Martin Wenig (2008) "The Effect of the Radio Wave Propagation Model in Mobile Ad Hoc Networks" Proceedings of World Academy of Science, Engineering And Technology Volume 36, pp 67-89, December 2008 ISSN 2070-3740

Ayyappan, K. Dananjayan, P. (2007) "Propagation Model for Highway in Mobile Communication System"

Baccelli, F. Błaszczyszyn, B. and M¨uhlethaler, P. (2006) "An Aloha Protocol for Multihop Mobile Wireless Networks," *IEEE Transactions on Information Theory*, Vol. 52, No. 2, pp. 421-436.

Backman, W. (2003) "*Error Correction on Predicted Signal levels in Mobile Communications"*, master thesis, 2003.

Balogun, J. (2000) "Impact of GSM on Economy and Development"

Bettstetter, C. (2004) "On the Connectivity of Ad Hoc Networks," *The Computer Journal, Special Issue on Mobile and Pervasive Computing*, Vol. 47, No. 4, pp. 432-447.

Carlson, A. B. Crilly, P. B.   Rutledge, J. C.   (2002) "*Communication Systems, An Introduction to Signal and Noise in Electrical Communication,*" 4th Edition, McGraw-Hill, 2002.

Clint smith, Daniel Collins (2000) "3G Wireless Network" page 136.

Domazetovic, A.   Greenstein, L. J.   Mandayan, N.   Seskar, I.   (2002) "*A New Modeling Approach 50 for Wireless Channels with Predictable Path Geometries,*" IEEE Beh. Tech. Conf.

Domazetovic, A.   Greenstein, L. J.   Mandayan, N.   Seskar, I.   (2002) "*A New Modeling Approach for Wireless Channels With Predictable Path Geometries,*" IEEE Beh. Tech. Conf.

Erceg, V. and Greenstein, L.J. (1999) *"*An Empirically Path Loss Model for Wireless Channels in Suburban Environments" IEEE Journal on Selected Areas of Communications, vol. 17,pp.1205-1211.

Erceg, V.; Greenstein, L.J.; Tjandra, S.Y.; Parkoff; S.R.; Gupta, A.; Kulic, B.; Julius, Bianchi, A.A.; (1999) "*An Empirical Based Path Loss Model for Wireless Channels in Suburban*

Environments," IEEE Journal on Selected Areas in Communications, vol. 17, Issue 7, pp. 1205-1211.

Erceg, V.; Greenstein, L.J.; Tjandra, S.Y.; Parkoff; S.R.; Gupta, A.; Kulic, B.; Julius Bianchi, A.A. (1999) "*An empirical based path loss model for wireless channels in suburban environments,*" IEEE Journal on Selected Areas in Communications, vol. 17, Issue 7, pp. 1205-1211.

Gibson JD (ed.) (1999) "*The Mobile Communications Handbook"*, 2nd edn.

Gordon L. Stüber (2001) "*Principle of Mobile Communication,*" 2nd Edition, Kluer Academic Publisher.

Gordon L. Stüber(2001) "*Principle of Mobile Communication,*" 2nd Edition, Kluer Academic Publisher.

Haenggi, M. (2009) "Outage, Local Throughput, and Capacity of Random Wireless Networks," accepted to *IEEE Transactions on Wireless Communications*. Available at http://www.nd.edu/~mhaenggi/pubs/twc09.pdf.

Hata, M. (1981) "Empirical formula for propagation loss in land mobile radio services," *IEEE Transactions on Vehicular Technology*, vol. vol. VT-29, pp. 317–325.

Hata, M. Nagatsu, T. (1980) "*Mobile Location Using Signal Strength Measurement in Cellular Systems,*" IEEE Trans. Veh. Tech., vol. 29, pp. 245-251.

http://www.allafrica.com (2009) "Nigeria Telecom Investment in the Country Hits U_S_18billion", Retrieved

Hung Huy Khong, Bing W. Kwan, Leonard J. Tung (2008) "*A Physics-Based Path-Loss Model for UWB (Ultra Wide-Band) Systems,*" Proc. International Conference on Wireless Networks (ICWN).

International Engineering Consortium (2005). Global System for Mobile Communication (GSM), IEEE Vol.5,No 23 pp.56-70

ITU (2009) "What Really is a Third Generation (3G) Mobile Technology" IEEE Vol.6,No 28 pp.57-87

Kagan, A. M. Linnik, Y. V. and Rao, C. R. (1973)"*Characterization Problems in Mathematical Statistic"*, Wiley.

King, R. J. (1969)"Electromagnetic Wave Propagation over a Constant Impedance Plane," Radio Science, vol. 4, pp. 255[268.

Lee, W. C. Y. (1999) "*Mobile Communications Design Fundamental,*" Indianapolis, IN: Sams.

Lee, W. C. Y., (1993) "Mobile Communications Fundamentals" Second Edition.

Lee, W.C.Y. (1998) "Mobile Communications Engineering" McGraw-Hill

Leveque, O. and Tse, D. (2007) "Hierarchical Cooperation Achieves Optimal Capacity Scaling in Ad Hoc Networks," *IEEE Transactions on Information Theory*, Vol. 53, No. 10, pp. 3549-3572.

Li, H.-J. Chen, C.-C. Liu, T.-Y. Lin, H.-C. (2000) "*Applicability of Ray-Tracing Techniques for Prediction of Outdoor Channel Characteristics,*" IEEE Trans. Veh. Tech.; pp. 2336-2349.

Li, H.-J. Chen, C.-C. Liu, T.-Y. Lin, H.-C. (2000)"*Applicability of Ray-Tracing Techniques for Prediction of Outdoor Channel Characteristics,*" IEEE Trans. Veh. Tech.; pp. 2336-2349.

Li, R. (2000) "The Accuracy of Norton's Empirical Approximations for Ground Wave Attenuation," IEEE Trans. Ant. Prop, vol. 31, pp. 624{628.

Lichun, L. (2000) "IEEE Ant. Prop. Magazine", pp. 21-33.

Longley, A.G, (1998) "Radio Propagation In Urban Area" OT Report New York. Pp. 78-144.

McKown, J. W. and Hamilton, R. L. (2001) *"Ray Tracing as a Design Tool for Radio Network,"* IEEE Network, pp. 27-30.

Medeisis, A. and Kajackas, A. (2000) *"On the Use of the Universal Okumura-Hata Propagation Prediction Model in Rural Areas"*, IEEE Vehicular Technology Conference Proceeding, Vol. 3, pp. 450-453.

Nigerianbusinessinfo.com (2003) "Revisiting Nigeria's Telecommunication Industry; Retrieved May 12, 2009.

Norton, K. A. (1936) "The Propagation of Radio Waves over the Surface of the Earth," Proc. Of the IRE, vol. 24, pp. 1367{1387.

Patwari, N. Hero, I. Perkins, A. O. M. Correal, N. and Dea, R. O (2003) "Relative Location Estimation in Wireless Sensor Networks," *IEEE Transactions on Signal Processing*, Vol. 51, No. 8, pp. 2137-2148.

Rappaport, T. S. (2002)*"Wireless Communications Principles and Practice"*, Prentice Hall.

Remley, K. A. Anderson, H. R. Weisshar, A. (2000) *"Improving the Accuracy of Ray-Tracing Techniques for Indoor*

Propagation Modeling," IEEE Trans. Veh. Tech., pp. 2350-2358.

Saunders, S. (2000) "*Antennas and Propagation for Wireless Communication Systems*", Wiley, 409 p.

Schaubach, K. R. Davis IV, Rappaport, T. S. (1992) "*A Ray Tracing Method for Predicting Path Loss and Delay Spread in Microcellular Environments,*" IEEE Veh. Trans. Tech., pp. 932-935.

Sharma, H.K. Sahu, S. and Sharma, S. (2011) "Enhanced Cost231 W.I. Propagation Model in Wireless Network" International Journal of Computer Applications, volume 19- No 6.

Sharma, P.K. (2013) International journal of Engineering Science and Technology, Vol.2(6), 2010, 2008-2013.

Sommerfeld, A. N. (2000)"Propagation of Waves in Wireless Telegraphy II," Ann. Phys., vol. 81, pp. 1135{1153.

Srinivasa, S. and Haenggi, M. (2007) "Modeling Interference in Finite Uniformly Random Networks," *International Workshop on Information Theory for Sensor Networks (WITS '07)*, Santa Fe.

Thiago, H, (2001), "A System For Propagation Analysis In Mobile Communication Environments" Institute Nacional De Telecommunicacoes, Voll. 04. No.2.

Turkmani, A.M.D and Toledo, A.F, (2002) "Propagation Into And Within Buildings At 900MHZ and 1400MHZ" Proceeding Of The 4th International Conference On Land Mobile Radio, New York. Pp.125-132.

Vaughan, R. Bach and Andersen, J. (2003) "*Channels Propagation and Antennas for Mobile Communications*" IEE, 753 p.

Wait, J. (1998) "The Ancient and Modern History of Electromagnetic Ground Wave Propagation," IEEE Ant. Prop. Magazine, pp. 7-24.

Zhao, X. Razoumov, L. and Greenstein, L. J (2004) "Path Loss Estimation Algorithms and Results for RF Sensor Networks," *Vehicular Technology Conference*, Vol. 7, pp. 4593-4596.